

1 **Early-life stress triggers long-lasting organismal resilience and longevity via tetraspanin**

2

3 Wei I. Jiang¹, Henry De Belly^{1, 2}, Bingying Wang¹, Andrew Wong¹, Minseo Kim¹, Fiona Oh¹,

4 Jason DeGeorge¹, Xinya Huang³, Shouhong Guang³, Orion D. Weiner^{1, 2}, Dengke K. Ma^{1, 4, 5,*}

5

6 ¹Cardiovascular Research Institute, University of California, San Francisco, San Francisco, USA

7 ²Department of Biochemistry and Biophysics, University of California, San Francisco, San

8 Francisco, CA, USA

9 ³The USTC RNA Institute, Division of Life Sciences and Medicine, Department of Obstetrics and

10 Gynecology, The First Affiliated Hospital of USTC, Biomedical Sciences and Health Laboratory

11 of Anhui Province, University of Science and Technology of China, Hefei, Anhui, China

12 ⁴Department of Physiology, University of California, San Francisco, San Francisco, CA, USA

13 ⁵Innovative Genomics Institute, University of California, Berkeley, Berkeley, CA, USA.

14

15 * Correspondence: Dengke.Ma@ucsf.edu (D.K.M.)

16

17 **Short title:** Mild Early-life Stress Extends Lifespan via Tetraspanin

18 **Teaser:** Studies reveal mechanisms of how early-life heat exposure produces long-lasting

19 benefits on longevity in the nematode *C. elegans*.

1 **Abstract**

2 Early-life stress experiences can produce lasting impacts on organismal adaptation and fitness.
3 How transient stress elicits memory-like physiological effects is largely unknown. Here we show
4 that early-life thermal stress strongly up-regulates *tsp-1*, a gene encoding the conserved
5 transmembrane tetraspanin in *C. elegans*. TSP-1 forms prominent multimers and stable web-
6 like structures critical for membrane barrier functions in adults and during aging. The up-
7 regulation of TSP-1 persists even after transient early-life stress. Such regulation requires CBP-
8 1, a histone acetyl-transferase that facilitates initial *tsp-1* transcription. Tetraspanin webs form
9 regular membrane structures and mediate resilience-promoting effects of early-life thermal
10 stress. Gain-of-function TSP-1 confers marked *C. elegans* longevity extension and thermal
11 resilience in human cells. Together, our results reveal a cellular mechanism by which early-life
12 thermal stress produces long-lasting memory-like impact on organismal resilience and longevity.

1 **Introduction**

2 Epidemiological and clinical studies in humans show that life stress of various forms can
3 exert profound lasting impacts on mental and physical health outcomes and lifespans (1–4). For
4 example, severe nutritional stress early in life can incur lifespan costs while psychosocial early-
5 life stress increases vulnerability to psychiatric disorders (5–7). By contrast, milder physiological
6 stresses, such as fasting with adequate nutrition or thermal stimuli via sauna exposure, are
7 associated with long-lasting health benefits (8, 9). Transient periods of stress can induce
8 persistent changes in the endocrine response, epigenetic regulation of gene expression and
9 plasticity changes in various organs (10–12). However, the underlying molecular and cellular
10 mechanisms by which transient early-life stress can produce memory-like physiological effects
11 remain poorly understood. Additionally, it is challenging to establish causal relationship between
12 putative cellular mechanisms and long-term health outcomes in human studies.

13 The free-living nematode *Caenorhabditis elegans* has emerged as a tractable model
14 system to study how early-life stress may affect adult phenotypes. Early-life exposure to
15 starvation, anoxia or osmotic stresses in *C. elegans* induces the transition into an L1 arrested
16 developmental stage or stress-resistant dauer stage, which can persist until environmental
17 conditions become favorable (13–15). Adults that have undergone the dauer stage preserve a
18 memory of their early-life starvation experience, resulting in alterations in gene expression,
19 extended lifespan, and decreased reproductive capacity (16, 17). Early-life starvation
20 experience can also reorganize neuronal modulation of stage-specific behavioral responses to
21 stresses (18). In addition, a one-day shift from 20 °C to 25 °C during early adulthood in *C.*
22 *elegans* appears to improve stress resistance and extend lifespan through known stress-
23 responding transcription factors: DAF-16, HSF-1, and HIF-1 (19, 20). It remains unclear how
24 specific effectors of these transcription factors, or other epigenetic mechanisms independent of
25 these factors, may elicit long-lasting impacts on adult stress resilience and longevity.

1 In this study, we use a robust thermal stress paradigm in *C. elegans* to uncover causal
2 mechanisms by which transient stress may exert lasting impacts on organismal resilience and
3 longevity. We show that transient heat exposure at 28 °C during late larval development
4 activates the gene *tsp-1*, which encodes a *C. elegans* homolog of the evolutionarily conserved
5 tetraspanin protein family. TSP-1 proteins form tetraspanin web-like structures and are essential
6 for maintaining membrane permeability, barrier functions, and heat-induced organismal
7 resilience and longevity. Initial induction of *tsp-1* by heat requires the histone acetyltransferase
8 CBP-1; however, surprisingly, this results in sustained up-regulation of TSP-1 protein without a
9 corresponding increase in mRNA abundance. We propose that the stability of the tetraspanin
10 web-like structure, achieved through TSP-1 multimerization, mediates the long-lasting
11 organismal impact triggered by transient mild thermal stress in early life.

12

13 **Results**

14 Using RNA-seq, we previously identified *tsp-1* as one of the genes highly up-regulated
15 by cold-warming (CW) stress (transient exposure to 4 or -20 °C followed by recovery at 20 °C) in
16 *C. elegans* (21–23). We generated translational reporters by fusing GFP with endogenous
17 regulatory DNA sequences (promoter and coding regions) for many of the CW stress-inducible
18 genes to monitor their induction kinetics and protein localization in live *C. elegans* during
19 development and adult responses to stresses. We focus on *tsp-1* in this study as the
20 constructed *tsp-1p::tsp-1::GFP* translational reporter shows robust and striking induction at L4
21 stages by not only CW stresses, but also mild heat stress at 25 °C, more so at 28 °C, less so at
22 20 °C or above 32 °C (**Fig. 1A, B; fig. S1**). Induction by 28 °C is heat-duration dependent (**fig.**
23 **S1**) and does not require HSF-1 (heat shock factor) (**fig. S2**) that mediates the canonical heat
24 shock response in *C. elegans* (24–28). By contrast, the heat-shock chaperon gene *hsp-16* is

1 also induced by 28 °C and requires HSF-1 for heat induction (**fig. S2**). These results highlight a
2 previously unknown, HSF-independent thermal induction of TSP-1 in *C. elegans*.

3 TSP-1 is a *C. elegans* homolog of the evolutionarily conserved tetraspanin protein family
4 in eukaryotes (29–31), predicted to form four-transmembrane α -helical segments and two
5 extracellular loop domains (**Fig. 1C**). We fused GFP to the C-terminus of TSP-1, leaving the N-
6 terminus of TSP-1 intact, which contains the first transmembrane helix targeting TSP-1 to
7 plasma membranes (**Fig. 1C**). Tetraspanins are versatile scaffolding transmembrane proteins,
8 specific members of which can interact with themselves to form multimers and control the
9 spatial organization of membrane lipids and proteins in networks called tetraspanin webs or
10 tetraspanin-enriched microdomains (29–31). We used sodium dodecyl-sulfate polyacrylamide
11 gel electrophoresis (SDS-PAGE) and native PAGE to analyze the thermal induction and
12 multimerization of TSP-1::GFP (**Fig. 1D**). Under baseline conditions at 20 °C, TSP-1::GFP
13 formed protein species corresponding to predicted monomers, SDS-resistant dimers and trimers
14 (in molecular weights). Heat at 28 °C for 24 hrs drastically increased all TSP-1::GFP species in
15 SDS-PAGE, and native PAGE further revealed the formation of high molecular-weight species
16 larger than dimers and trimers (**Fig. 1D**). Confocal microscopy revealed that TSP-1::GFP was
17 highly enriched along the apical membrane of intestinal cells (**Fig. 1E**). Heat at 28 °C for 72 hrs
18 or a transient period of 24 hrs starting from L4 markedly increased the abundance of TSP-
19 1::GFP, forming tetraspanin web-like structures discernable at high resolution (**Fig. 1E**). Such
20 structures were not caused by temperature effect on the tag GFP *per se* since intestinal apical
21 membrane-tethered GFP alone did not show such a pattern (**fig. S3**). In addition, *tsp-1*
22 endogenously tagged with a worm-codon optimized fluorescent protein wrmScarlet by
23 CRISPR/Cas showed similar up-regulation by heat at 28 °C and formation of tetraspanin web-
24 like structures (**fig. S4**). Compared with multi-copy transgenic TSP-1::GFP, endogenously

1 tagged TSP-1::wrnScarlet exhibited overall weaker fluorescent intensity and enabled us to
2 better resolve finer tetraspanin webs with regular lattice-like structures (**fig. S4F-I**).

3 Tetraspanin has been implicated in numerous biological processes, yet its precise
4 cellular functions remain largely unknown. We next sought to determine normal TSP-1
5 expression pattern under non-stress conditions and its adult physiological function during aging
6 in *C. elegans*. At day 1 (young adult), 5 (adult), and 9 (old adult) post L4 stages, TSP-1::GFP
7 exhibited a progressive increase in abundance (**Fig. 2A-E**). Cultivation at 25 °C accelerated the
8 time-dependent increase of TSP-1::GFP abundance, albeit to a lesser degree than a transient
9 24 hrs period at 28 °C (**Fig. 2A-E, Fig. 1E**) (28 °C represents harsh stress precluding chronic
10 analyses of TSP-1::GFP at day 5 and 9 because of organismal death by prolonged exposure,
11 see below). The striking tetraspanin web-like structure formed by TSP-1::GFP (**Fig. 1E**)
12 prompted us to test the role of TSP-1 in maintaining membrane integrity. We developed a
13 fluorescein-based assay modified from our previous studies (21) to measure the acute barrier
14 function or permeability of intestinal membranes in *C. elegans* (**Fig. 2F**). In wild-type animals, a
15 short (10 min) incubation with fluorescein did not result in detectable fluorescence signals in the
16 intestine (**Fig. 2G**). By contrast, the same procedure led to a dramatic accumulation of
17 fluorescein in the intestine of *tsp-1* deficient animals (**Fig. 2G-2J**). This difference was notable at
18 the L4 stage and particularly prominent in adults at day 5 post L4 (**Fig. 2J**). We observed similar
19 defects in membrane barrier functions using RNA interference (RNAi) against two different
20 coding regions of *tsp-1* (**fig. S5**). These results indicate that TSP-1 up-regulation during aging or
21 by thermal stress may physiologically maintain intestinal barrier functions.

22 We characterized how early-life thermal stress (ELTS, 28 °C for 24 hrs starting from L4
23 stages) may trigger lasting TSP-1::GFP expression. In control animals at 20 °C, TSP-1::GFP
24 remained at low baseline levels largely unaltered for the first 48 hrs and became slightly
25 elevated at 72 hrs (**Fig. 3A**). By contrast, ELTS (28 °C for 24 hrs at L4) triggered robust up-

1 regulation of TSP-1::GFP abundance at 24 hrs post L4, which remained still high at 20 °C even
2 for another 24 and 48 hrs after the initial ELTS (**Fig. 3A**). Chronic exposure to 28 °C starting at
3 L4 induced stronger expression of TSP-1::GFP for 48 hrs than 24 hrs, but reached peak levels
4 at 72 hrs (**Figs. 3B, C**). We took advantage of the robust TSP-1::GFP activation by ELTS and
5 performed RNAi screens for genes that are required for TSP-1::GFP up-regulation. Given the
6 importance of transcription factors and histone modifying enzymes in epigenetic gene regulation
7 (32–34), we assembled a customized library of RNAi clones targeting >100 genes with
8 adequate expression in the intestine (transcript per million >2) and that encode proteins
9 including stress-responding transcription factors and chromatin/epigenetic regulators (**Fig. 3D**,
10 **table S1**). From such candidate screens, using RNAi vector only as negative control and *tsp-1*
11 RNAi as a positive control, we found that RNAi against only one hit, *cbp-1*, robustly prevented
12 TSP-1::GFP up-regulation by ELTS (**Fig. 3E, 3F**). *cbp-1* encodes the *C. elegans* ortholog of
13 histone acetyltransferase p300/CBP that promotes gene transcription (35–43). RNAi against
14 many of the known genes encoding heat-responding transcription factor, including *hsf-1*, *hsf-2*,
15 *hif-1* and *nhr-49*, did not block TSP-1::GFP up-regulation (**table S1**). Although TSP-1::GFP
16 remained high for 24 and 48 hrs at 20 °C post initial ELTS (**Fig. 3C**), qRT-PCR measurements
17 revealed that the up-regulation of *tsp-1* mRNA transcripts by 28 °C was transient but not
18 sustained, and required CBP-1 (**Fig. 3F**). These results indicate that transient ELTS can trigger
19 lasting up-regulation of TSP-1 abundance, which requires initial CBP-1-dependent *tsp-1*
20 transcription but remains stable even after *tsp-1* expression has normalized after ELTS.

21 We aimed to determine the subcellular localization and stability of the heat-induced TSP-
22 1 tetraspanin web formation. We generated strains with CRISPR-mediated wrmScarlet knock-in
23 at the endogenous *tsp-1* locus that was genetically crossed with previously validated GFP
24 reporters for intestinal subcellular structures, including Akt-PH::GFP that binds to PIP2/PIP3 at
25 the inner leaflet of plasma membranes, or GFP::C34B2.10(SP12) that labels the endoplasmic

1 reticulum membrane (ERm) (21, 44, 45). Confocal microscopic imaging revealed the proximity
2 of Akt-PH::GFP and TSP-1::wrnScarlet throughout intestinal apical membranes (**Fig. 4A**),
3 corroborated by quantitative fluorescent intensity correlation analysis (**Fig. 4B**). By contrast,
4 ERm::GFP and TSP-1::wrnScarlet did not exhibit apparent co-localization (**Fig. 4C, 4D**). We
5 further assessed the temporal dynamics of tetraspanin webs by imaging endogenous TSP-
6 1::wrnScarlet (**Fig. 4E**) and found that the tetraspanin web structure exhibited markedly
7 consistent stability across the entire field and time scale of imaging (**Fig. 4F, Movie S1**). These
8 results indicate that TSP-1-dependent tetraspanin webs, once induced by heat, form rather
9 stable structures closely associated with the intestinal apical membrane.

10 Next, we investigated the consequences of TSP-1 up-regulation triggered by ELTS at
11 the organismal level. To address this, we measured the population lifespan and survival rates of
12 wild type and *tsp-1* deletion mutants under various heat stress conditions. Under constant 28 °C
13 starting from L4, deficiency of *tsp-1* caused shortened lifespan and premature population death
14 compared with wild-type animals (**Fig. 5A**). Transient ELTS (28 °C for 24 hrs at L4) extended
15 the longevity of wild-type animals at subsequent normal cultivation temperature (20 °C). By
16 contrast, the ELTS effect on longevity extension was abolished in *tsp-1* mutants (**Fig. 5B**). We
17 applied 28 °C exposure to animals growing constantly for 48 hrs at 20 °C post L4, and found
18 that transient ELTS (28 °C for 24 hrs at L4) enhanced survival rates in wild type but not *tsp-1*-
19 deficient animals (**Fig. 5C**). We used RNAi against *cbp-1* (null mutations are lethal) and
20 observed that reducing *cbp-1* expression caused even more shortened population lifespans
21 (**Fig. 5D**). Given the more severe phenotype of *cbp-1* deficiency, CBP-1 likely regulates
22 additional genes beyond *tsp-1*. Indeed, we found that the heat shock chaperon-encoding gene
23 *hsp-16* was transiently induced by ELTS, and its induction required both HSF-1 and CBP-1 (**fig. S6**).
24 Unlike *hsp-16*, ELTS induction of *tsp-1* is HSF-1 independent (**fig. S2**), yet its similarly
25 transient induction leads to stable tetraspanin multimerization and web-like structural formation

1 (Fig. 3). Finally, we used a CRISPR-mediated GFP knock-in allele of *cbp-1* to show that ELTS
2 markedly increased the probability of nuclear entry by endogenous CBP-1 in the intestine,
3 suggesting that CBP-1 plays an instructive (actively mediating the effect of heat) rather than
4 permissive (gate-keeping to allow heat effect) role in *tsp-1* up-regulation by heat (Fig. 5E, F).
5 Like induction of *tsp-1* mRNAs but not TSP-1 proteins, increased nuclear entry of CBP-1 also
6 followed a similarly transient pattern upon ELTS (fig. S7, Fig. 3). Taken together, these results
7 demonstrate that TSP-1 promotes survival under 28 °C heat stress and its CBP-1-dependent
8 induction mediates effects of transient ELTS on lasting benefits to longevity and organismal
9 resilience to subsequent heat stress conditions (Fig. 5G).

10 To assess the sufficiency of TSP-1 in conferring stress resilience, we determined the
11 gain-of-function effects of TSP-1 in *C. elegans* and ectopically in human cells. In *C. elegans*, we
12 generated two transgenic strains carrying genomic *tsp-1* regions as extrachromosomal arrays at
13 either low or high copy numbers (over-expression or OE, line 1 and 2, respectively) (Fig. 6A).
14 qRT-PCR confirmed that *tsp-1* mRNA expression levels are differentially up-regulated in the two
15 strains with array-positive animals (Fig. 6A). In thermal resilience assays, we found that OE line
16 2 with high-copy *tsp-1* arrays exhibited markedly enhanced survival rates upon continuous 28
17 °C heat stress, compared with array-negative control or OE line 1 with low-copy *tsp-1* arrays
18 (Fig. 6B). In lifespan assays, OE line 2 exhibited similarly extended survival and longevity under
19 20 °C cultivation conditions, with a marked increase in both median (63%) and maximal (24%)
20 lifespans in animals carrying high-copy expression of *tsp-1* (Fig. 6C). Furthermore, to assess
21 the gain-of-function effect of TSP-1 in a heterologous cellular context, we over-expressed *C.*
22 *elegans* *tsp-1* cDNA with a tagged *GFP* driven by the CMV promoter in human embryonic
23 kidney cell lines (HEK293) (Fig. 6D). Such ectopic expression of *tsp-1* resulted in prominent
24 tetraspanin web-like structures (Fig. 6E) and functionally protected HEK293 cells against

1 thermal stress conditions (42 °C). These results demonstrate striking gain-of-function effects of
2 tetraspanin-encoding *tsp-1* in both *C. elegans* and heterologous mammalian cells.

3

4 **Discussion**

5 Previous studies have shown that mild and transient metabolic or environmental stress
6 in early life can produce beneficial effects, extending longevity in *C. elegans* (38, 46–51). While
7 heat exposure activates numerous genes involved in proteostasis and defense responses,
8 specific HSF-independent target genes with causal effects on longevity remain unidentified. In
9 this work, we identify *tsp-1* as a heat-inducible gene that mediates effects of ELTS on
10 organismal resilience and longevity. Regulatory mechanisms governing how heat stress
11 activates CBP-1 in coordination with other unidentified factors await further exploration. Our
12 data suggest that *tsp-1* expression leads to TSP-1 protein multimerization and the formation of
13 stable tetraspanin web structures, which persist even in the absence of initial stimuli and *tsp-1*
14 transcript up-regulation. This tetraspanin web-based stable protein structure formation
15 represents a novel mechanism of cellular memory, distinct from previously known modes of
16 epigenetic regulation primarily occurring in the nucleus, such as DNA and histone modifications.

17 We demonstrate that TSP-1 is crucial for maintaining intestinal membrane barrier
18 functions and enhancing animal adaptation and survival under heat-stress conditions and during
19 aging. The *C. elegans* genome encodes 21 tetraspanin family proteins, including *tsp-1* and *tsp-2*
20 located in the same operon, which may be similarly regulated by heat. Other tetraspanin family
21 members have been implicated in plasma membrane repair, extracellular vesicle formation, and
22 oxidative stress responses (52–55). It is plausible that different tetraspanins may be regulated in
23 a tissue-specific, developmental stage-specific, and stress-specific manner to confer distinct
24 biological functions. In addition to heat that impacts membrane barrier and integrity, other types

1 of specific membrane-perturbing stress can also induce *tsp-1* expression through CBP-1, which
2 likely regulates additional transcriptional targets that together safeguard intestinal barrier
3 functions (fig. S8, 9). Several mammalian tetraspanins have been shown to play important roles
4 in maintaining blood-brain or retina-blood barriers in endothelial cells and attenuating
5 inflammation, cell senescence, and organismal aging (56–58). Thus, we propose that the
6 functional roles of tetraspanins are evolutionarily conserved, likely mediating long-lasting effects
7 of transient cellular and organismal stresses in mammals, including humans.

1 **Materials & Methods**

2

3 ***C. elegans* strains**

4 *C. elegans* strains were grown on nematode growth media (NGM) plates seeded with *Escherichia*
5 *coli* OP50 at 20°C with laboratory standard procedures unless otherwise specified. The N2 Bristol
6 strain was used as the reference wild type (59). Mutants and integrated transgenes were back-
7 crossed at least 5 times. Genotypes of strains used are as follows: *dmals125* [*tsp-1p::tsp-1::GFP*;
8 *unc-54p::mCherry*], *dmals8* [*hsp-16p::GFP*; *unc-54p::mCherry*]; *him-5(e1490)*, *hjls14* [*vha-*
9 *6p::GFP::C34B2.10(SP12 ER membrane) + unc-119(+)*], *etEx2* [*glo-1p::GFP::ras-2 CAAX + rol-*
10 *6*], *tsp-1(ok3594)*, *hsf-1(sy441)*, *tsp-1(syb7456[tsp-1::wrmscarlet])*, *cbp-1(ust475[GFP::cbp-1])*.

11 For CRISPR knock-in of *cbp-1* with 3xFLAG::GFP::cbp-1, a *cbp-1* promoter region was
12 PCR-amplified with the primers 5'- gggtaacgcccagCACGTGtgggctgactcgtgctg -3' and 5'-
13 ccgtcatggtcttgtagtctggtggttcatccatcaattagta -3' from N2 genomic DNA. A *cbp-1* coding
14 sequence region was PCR amplified with the primers 5'-
15 AAGGAGGTGGAGGTGGAGCTatggatgaaccaccatcaa -3' and 5'-
16 cagcggataacaatttacaaatgcacatggatccacc -3' from N2 genomic DNA. A 3xFLAG::GFP region
17 was PCR-amplified with the primers 5'- gactacaaagaccatgacgg -3' and 5'-
18 AGCTCCACCTCCACC -3' from SHG1890 genomic DNA. ClonExpress MultiS One Step
19 Cloning Kit (Vazyme C113-02, Nanjing) was used to connect these fragments with vector
20 amplified with 5'- tgtgaaattgttatccgctgg -3' and 5'- caCACGTGctggcgttacc -3' from L4440. The
21 injection mix contained pDD162 (50 ng/ul), *cbp-1* repair plasmid (50 ng/ul), pCFJ90 (5 ng/ul),
22 and three sgRNAs (30 ng/ul). The mix was injected into young adult N2 animals, and the coding
23 sequence of 3xFLAG::GFP was inserted after the start codon using the CRISPR/Cas9 system.
24 The *tsp-1::wrmscarlet* knock-in allele was generated similarly (Sunybiotech), with *wrmScarlet*
25 sequences inserted before the termination codon of *tsp-1* in the N2 background.

1 For overexpression of *tsp-1* (3.26 kb), the *tsp-1* promotor (1.98 kb) and 1,283 bp
2 genomic DNA fragment of *tsp-1* coding region was PCR-amplified with the primers 5'-
3 aataataattcagggatgtggtctcaa -3' and 5'- tgacaagggtactgttagttcgct -3' from N2 genomic DNA.
4 The injection mix contained *tsp-1p::tsp-1* (10-50 ng/μl) and *unc-54p::GFP* (25 ng/μl) to establish
5 transgenic strains carrying extrachromosomal arrays of varying copy numbers.

6

7 **Compound and confocal imaging**

8 Epifluorescence compound microscopes (Leica DM5000 B Automated Upright Microscope
9 System) were used to capture fluorescence images (with a 10× objective lens). Animals of
10 different genotypes and different stages (L4, Day1, Day5, Day9) and different heat treatment were
11 randomly picked and treated with 10 mM sodium azide solution (71290-100MG, Sigma-Aldrich)
12 in M9, aligned on an 2% agarose pad on slides for imaging. The same settings (for bright-field:
13 exposure time 1 second, for GFP: exposure time 10 seconds) were maintained for the images of
14 all samples. The integrated density (IntDen) of TSP-1::GFP was measured by NIH image program
15 (Fiji image J) , average of mean gray value (three background area of each image randomly
16 selected) were employed to normalized the TSP-1::GFP. For confocal images, the worms were
17 randomly chosen and treated with 10 mM sodium azide in M9 solution and aligned on an 2%
18 agarose pad on slides and images acquired using a confocal microscope (Leica TCS SPE) with
19 a 63× objective lens, the same settings were maintained for the images of all samples. Imaging
20 in Figure 4 was conducted under room temperature conditions using a Nikon Eclipse Ti inverted
21 microscope equipped with a Borealis beam conditioning unit (Andor), a CSU-W1 Yokogawa
22 spinning disk (Andor; Belfast, Northern Ireland), a 100X PlanApo TIRF 1.49 numerical aperture
23 (NA) objective (Nikon; Toyko, Japan), an iXon Ultra EMCCD camera (Andor), and a laser merge
24 module (LMM5, Spectral Applied Research; Exton, PA) containing 405, 440, 488, and 561-nm

1 laser lines. Micro-Manager (UCSF) was used to control all the hardware. Fiji (NIH) (60) and Prism
2 (Graphpad software, Inc) were used for image display and co-localization analysis.

3

4 **SDS-page and native-page western blotting**

5 For SDS-PAGE samples, stage-synchronized animals for control and experiment groups were
6 picked (n = 50) in 60 µl M9 buffer and lysed directly by adding 20 µl of 4x Laemmli sample buffer
7 (1610747, Bio-Rad) contain 10% of 2-Mercaptoethanol (M6250-100ML, Sigma(v/v)). Protein
8 extracts were denatured at 95 °C for 10 min and separated on 10% SDS-PAGE gels (1610156,
9 Bio-Rad) at 80 V for ~40 min followed by 110 V for ~70 min. The proteins were transferred to a
10 nitrocellulose membrane (1620094, Bio-Rad,) at 25 V for 40 mins by Trans-Blot® Turbo™
11 Transfer System (Bio-Rad). The NC membrane was initially blocked with 5% nonfat milk and 2%
12 BSA (A4503, Sigma (v/v)) in tris buffered saline with 0.1% Tween 20 (93773, Sigma) (TBS-T) at
13 room temperature for 1 h. Proteins of interest were detected using antibodies against GFP (A6455,
14 Invitrogen) and Histone H3 (ab1791, Abcam) in cold room for overnight. After three washes of 5
15 min each with tris-buffered saline with 0.1% Tween 20, anti-rabbit IgG, HRP-linked Antibody
16 (7074S, Cell Signaling Technology) was added at a dilution of 1:5000.

17 For native-PAGE samples, stage-synchronized animals were washed down from NGM
18 plates using M9 solution and subjected to 850 g for 60 seconds, and the pellet animals were
19 resuspended in pre-cooled 300 µl lysis buffer (M9 buffer + Protein inhibitors cocktails, A32965,
20 Thermo Fisher), then lysed by TissueRuptor (Motor unit '6') for 10 seconds and taken out,
21 repeated 3-5 times, followed by diluting the samples with Native Sample Buffer (161-0738, Bio-
22 Rad). Proteins were resolved by 4–15% Mini-PROTEAN® TGX™ Precast Protein Gels (4561086,
23 Bio-Rad,) and transferred to a nitrocellulose membrane (1620094, Bio-Rad). The NC membrane
24 was initially blocked with 5% nonfat milk and 2% BSA (A4503, Sigma (v/v)) in Tris buffered saline

1 with 0.1% Tween 20 (93773, Sigma) (TBS-T) at room temperature for 1 h. native TSP-1::GFP
2 were detected using antibodies against GFP (1:1000, 66002-1-Ig, Proteintech) at cold room
3 overnight. After three washes of 5 min each with Tris-buffered saline with 0.1% Tween 20, goat
4 anti-Mouse IgG (H+L) Secondary Antibody [HRP] (NB7539, Novus) added at a dilution of 1:5000
5 as the secondary antibody.

6

7 **Fluorescein assay**

8 Stage-synchronized animals (L4, Day1 and Day5) of different genotypes at 20°C were randomly
9 picked to 20 µl M9 solution in 1.5 mL tube, followed by treatment with 100 µl of Fluorescein
10 (F0095-25G, TCI America, 10 mg/ml in M9 buffer) at room temperature for 10 minutes. Worms
11 were transferred to a NGM plate (without OP50), collected to new NGM plate with 200 µl M9
12 buffer to wash for three times, followed by randomly picking and treatment with 10 mM sodium
13 azide in M9 buffer and aligned on an 2% agarose pad on slides for compound microscope imaging.
14 The integrated density (IntDen) of fluorescein was measured by NIH image program (Fiji image
15 J), average of mean gray value (three background areas of each image randomly selected) was
16 employed to normalize the fluorescein signals.

17

18 **RNA interference (RNAi) cloning and screen**

19 To clone the *tsp-1* RNAi sequences, *tsp-1* exon 1-3 (Chr. III, C02F5.8, 1124 bp size, primer
20 forward: GGCGGCCGCTCTAGAACTAGTACAGATTTCTCCACCTCTTCC, primer reverse:
21 TCCACGCGTCACGTGGCTAGCATTCTAAATTTTCAGAGCCCACC) and exon 1-5 (Chr. III,
22 C02F5.8, 1472 bp size, primer forward:
23 GGCGGCCGCTCTAGAACTAGTTCCACCTCTTCCACCTTCATTAC, primer reverse:
24 TCCACGCGTCACGTGGCTAGCTGACAAGGGTACTGTAGTCGTCT) were PCR-amplified

1 from wild-type N2 gDNA and subcloned into the Spel and Nhel sites of a pL4440 expression
2 vector with NEBuilder® HiFi DNA Assembly Cloning Kit (E2621L, NEB). Briefly, PCR was
3 performed with the following protocol on a MyCycler™ Thermal Cycler (Bio-Rad): 98 °C for 30
4 s, 98 °C for 10 s, 55 °C for 30 s, 72 °C for 2 min (35 cycles); 72 °C for 5 min, and a final hold at
5 12 °C. The PCR products were analyzed on a 1.5 % agarose gel. 25 ng of precut pL4440 vector
6 with 2-fold excess of *tsp-1* PCR fragment (50 ng) were used for assembly in a thermocycler at
7 50°C for 30 minutes, 25 ng of precut pL4440 vector with same water instead of PCR fragment
8 were employed as native assembly control. 5 µl of assembly preparations were transformed to
9 NEB 5-alpha Competent *E. coli* (C2987H, NEB) by heat shock at exactly 42°C for exactly 30
10 seconds. Positive clones were verified by bacteria PCR by 2x thermo scientific dream taq green
11 PCR master mix (pL4440 forward: CTTATCGAAATTAATACG, pL4440 reverse:
12 AGGGCGAATTGGGTACCG). Positive pL4440-*tsp-1* RNAi plasmids were transformed to
13 competent HT115 by electroporation and verified the positive HT115 clones by bacteria PCR.

14 RNAi and screen for hits blocking TSP-1::GFP were performed by feeding worms with *E.*
15 *coli* strain HT115 (DE3) expressing double-strand RNA (dsRNA) targeting endogenous genes.
16 Briefly, dsRNA-expressing bacteria were replicated from the Ahringer library to LB plates
17 containing 100 µg/ml ampicillin (BP1760-25, Fisher Scientific) at 37 °C for 16 hrs. Single clone
18 was picked to LB medium containing 100 µg/ml ampicillin at 37 °C for 16 hrs and positive clones
19 (verified by bacteria PCR with pL4440 forward and pL4440 reverse primers) were spread onto
20 NGM plates containing 100 µg/ml ampicillin and 1 mM isopropyl 1-thio-β-Dgalactopyranoside
21 (IPTG, 420322, Millipore) for 24 hrs (namely RNAi plates). Developmentally synchronized
22 embryos from bleaching of gravid adult hermaphrodites were plated on RNAi plates and grown at
23 20 °C to L4 stage followed by transfer to 28 °C incubator for 24 hrs. Randomly selected population
24 was observed under the epifluorescence microscope (SMZ18, Nikon) with hits considered to
25 block TSP-1::GFP when observing GFP levels comparable to that by *tsp-1* RNAi (positive control).

1

2 **qRT-PCR**

3 Animals were washed down from NGM plates using M9 solution and subjected to RNA
4 extraction using TissueDisruptor and RNA lysis buffer (Motor unit '6' for 10 seconds and take it
5 out, repeat 3-5 times on ice) and total RNA was extracted following the instructions of the Quick-
6 RNA MiniPrep kit (Zymo Research, R1055) and reverse transcription was performed by
7 SuperScript™ III (18080093, Thermo scientific). Real-time PCR was performed by using
8 ChamQ Universal SYBR qPCR Master Mix (Q711-02, Vazyme) on the Roche LightCycler96
9 (Roche, 05815916001) system. Ct values of *tsp-1* were normalized to measurements of *rps-23*
10 (*C. elegans*) levels. Primer for qRT-PCR: *tsp-1* (forward, CTTGATTGCCGTTGGATT;
11 reverse, CCCAAAGAAAGGCCGATAAT), *hsp-16.2* (forward:
12 ACGTCCGTTTTGGTGATCTTAT; reverse, TCTGGTTAACTGTGAGACGTTG) and *rps-23*
13 (forward, CGCAAGCTCAAGACTCATCG; reverse, AAGAACGATTCCCTGGCGT).

14

15 **Thermal resilience and lifespan assays**

16 Animals were cultured under non-starved conditions for at least 2 generations before heat stress
17 assays. For treatment of “early-life thermal stress” (ELTS), bleach-synchronized eggs were
18 growth to the L4 stage at 20 °C, and populations were kept at 28 °C for 24 hrs and then recovered
19 for 0-72 hrs at 20 °C. For thermal resilience assays, stage-synchronized L4 stage worms (n > 30)
20 were picked to new NGM plates seeded with OP50 and transferred to 28 °C incubator. Animals
21 were scored for survival per 24 hrs. Worms failing to respond to repeated touch of a platinum wire
22 were scored as dead. For lifespan assays, stage-synchronized L4 stage worms (n = 50) were
23 picked to new NGM plates seeded with OP50 containing 50 µM 5-fluoro-2'-deoxyuridine (FUDR)

1 to prevent embryo growth at 20 °C incubator. Animals were scored for survival per 24 hrs. Worms
2 failing to respond to repeated touch of a platinum wire were scored as dead.

3

4 **Mammalian expression constructs for *C. elegans* TSP-1**

5 The *C. elegans* *tsp-1* open reading frame was PCR-amplified with the primers 5'-
6 GCGGCCTTAATTAAACCTCTAGAATGGCAACTTGGAAATTATCATACG -3' and 5'-
7 AGCTCGAGATCTGAGTCCGGcAAAACGAGTGTCCTCGGTGATG -3' from cDNA prepared
8 from heat-induced (T28 24 hrs) wild-type animals. GFP fragment was PCR-amplified with 5'-
9 gCCGGACTCAGATCTCGAGCTATGGTGAGCAAGGGCGCCG -3' and 5'-
10 CGGATCTTACTTACTTAGCGGCCGCTTACTTGTACAGCTCATCCATGCC -3' from the
11 pHAGE2-gfp plasmid. The *tsp-1*-GFP fragment was PCR-amplified using overlapping PCR and
12 sub-cloned by T4 DNA Ligase to the pHAGE2-gfp plasmid at the XbaI and NotI sites.

13

14 **HEK293T cells and thermal resilience assay**

15 Human embryonic kidney (HEK) 293T cells were maintained in Dulbecco's modified Eagle's
16 medium with 10% inactive fetal bovine serum and penicillin-streptomycin (Gibco, Grand Island,
17 15140122) at 37 °C supplied with 5% CO₂ in an incubator (Thermo Fisher Scientific) with a
18 humidified atmosphere. Cells were washed once using PBS and digested with 0.05% trypsin-
19 EDTA (Gibco) at 37 °C for routine passage of the cells. All HEK 293T cells were transiently
20 transfected with indicated constructions using the lipo2000 (1 mg/ml, LIFE TECHNOLOGIES)
21 reagent. The lipo2000/DNA mixture with the ratio of lipo2000 to DNA at 3:1 was incubated for 30
22 min at room temperature before being added to the HEK 293T cell cultures dropwise. For thermal
23 resilience assay, mock control and transfected HEK293T cells (48 h) in 24 well plate were placed
24 in a culture incubator with an ambient temperature at 42°C and humidified 5% CO₂ for 8 h

1 followed by cell death assay or imaging with 4% PFA treatment for 12 min at room temperature.
2 For cell death assay, the collected cells were resuspended with 100 μ l buffer with addition of 0.1
3 μ l Sytox blue (Thermo Fisher Scientific) for an additional 15 min at room temperature. 25 μ l of
4 incubated cells were loaded into ArthurTM cell analysis slide (Nanoentek, AC0050). The
5 fluorescence intensity was measured for individual cells using automated cytometry (ArthureTM
6 image based cytometer, Nanoentek, AT1000) by viability assay. The 226 RFU (Fluorescence)
7 threshold and cell size min 5 to max 25 were used for cell death analysis and quantification.

8

9 **Statistics**

10 Data were analyzed using GraphPad Prism 9.2.0 Software (Graphpad, San Diego, CA) 389 and
11 presented as means \pm S.D. unless otherwise specified, with P values calculated by unpaired
12 two-tailed t-tests (comparisons between two groups), one-way ANOVA (comparisons across
13 more than two groups) and two-way ANOVA (interaction between genotype and treatment), with
14 post-hoc Tukey HSD and Bonferroni's corrections. The lifespan assay was quantified using
15 Kaplan–Meier lifespan analysis, and P values were calculated using the log-rank test.

16

17 **References**

- 18 1. E. R. de Kloet, M. Joëls, F. Holsboer, Stress and the brain: from adaptation to disease. *Nat Rev
19 Neurosci* **6**, 463–475 (2005).
- 20 2. S. E. Taylor, B. M. Way, T. E. Seeman, Early adversity and adult health outcomes. *Dev Psychopathol
21* **23**, 939–954 (2011).
- 22 3. N. Fogelman, T. Canli, Early Life Stress, Physiology, and Genetics: A Review. *Front Psychol* **10**, 1668
23 (2019).
- 24 4. V. J. Felitti, R. F. Anda, D. Nordenberg, D. F. Williamson, A. M. Spitz, V. Edwards, M. P. Koss, J. S.
25 Marks, Relationship of childhood abuse and household dysfunction to many of the leading causes

1 of death in adults. The Adverse Childhood Experiences (ACE) Study. *Am J Prev Med* **14**, 245–258
2 (1998).

3 5. S. English, T. Uller, Does early-life diet affect longevity? A meta-analysis across experimental
4 studies. *Biol Lett* **12**, 20160291 (2016).

5 6. K. A. McLaughlin, K. C. Koenen, E. J. Bromet, E. G. Karam, H. Liu, M. Petukhova, A. M. Ruscio, N. A.
6 Sampson, D. J. Stein, S. Aguilar-Gaxiola, J. Alonso, G. Borges, K. Demyttenaere, R. V. Dinolova, F.
7 Ferry, S. Florescu, G. de Girolamo, O. Gureje, N. Kawakami, S. Lee, F. Navarro-Mateu, M. Piazza, B.-
8 E. Pennell, J. Posada-Villa, M. Ten Have, M. C. Viana, R. C. Kessler, Childhood adversities and post-
9 traumatic stress disorder: evidence for stress sensitisation in the World Mental Health Surveys. *Br J
10 Psychiatry* **211**, 280–288 (2017).

11 7. D. W. Brown, R. F. Anda, H. Tiemeier, V. J. Felitti, V. J. Edwards, J. B. Croft, W. H. Giles, Adverse
12 childhood experiences and the risk of premature mortality. *Am J Prev Med* **37**, 389–396 (2009).

13 8. V. D. Longo, M. P. Mattson, Fasting: molecular mechanisms and clinical applications. *Cell Metab*
14 **19**, 181–192 (2014).

15 9. T. Laukkanen, S. K. Kunutsor, H. Khan, P. Willeit, F. Zaccardi, J. A. Laukkanen, Sauna bathing is
16 associated with reduced cardiovascular mortality and improves risk prediction in men and women:
17 a prospective cohort study. *BMC Med* **16**, 219 (2018).

18 10. S. J. Lupien, B. S. McEwen, M. R. Gunnar, C. Heim, Effects of stress throughout the lifespan on the
19 brain, behaviour and cognition. *Nat Rev Neurosci* **10**, 434–445 (2009).

20 11. B. S. McEwen, In pursuit of resilience: stress, epigenetics, and brain plasticity. *Ann N Y Acad Sci*
21 **1373**, 56–64 (2016).

22 12. D. K. Ma, M.-H. Jang, J. U. Guo, Y. Kitabatake, M.-L. Chang, N. Pow-Anpongkul, R. A. Flavell, B. Lu,
23 G.-L. Ming, H. Song, Neuronal activity-induced Gadd45b promotes epigenetic DNA demethylation
24 and adult neurogenesis. *Science* **323**, 1074–1077 (2009).

25 13. P. A. Padilla, M. L. Ladage, Suspended animation, diapause and quiescence. *Cell Cycle* **11**, 1672–
26 1679 (2012).

27 14. N. O. Burton, T. Furuta, A. K. Webster, R. E. W. Kaplan, L. R. Baugh, S. Arur, H. R. Horvitz, Insulin-
28 like signalling to the maternal germline controls progeny response to osmotic stress. *Nat Cell Biol*
29 **19**, 252–257 (2017).

30 15. R. C. Cassada, R. L. Russell, The dauerlarva, a post-embryonic developmental variant of the
31 nematode *Caenorhabditis elegans*. *Dev Biol* **46**, 326–342 (1975).

32 16. S. E. Hall, M. Beverly, C. Russ, C. Nusbaum, P. Sengupta, A cellular memory of developmental
33 history generates phenotypic diversity in *C. elegans*. *Curr Biol* **20**, 149–155 (2010).

34 17. M. C. Ow, K. Borziak, A. M. Nichitean, S. Dorus, S. E. Hall, Early experiences mediate distinct adult
35 gene expression and reproductive programs in *Caenorhabditis elegans*. *PLoS Genet* **14**, e1007219
36 (2018).

1 18. R. Ali Nasser, Y. Harel, S. Stern, Early-life experience reorganizes neuromodulatory regulation of
2 stage-specific behavioral responses and individuality dimensions during development. *Elife* **12**,
3 e84312 (2023).

4 19. J. Huang, K. Wang, M. Wang, Z. Wu, G. Xie, Y. Peng, Y. Zhang, X. Zhang, Z. Shao, One-day thermal
5 regime extends the lifespan in *Caenorhabditis elegans*. *Comput Struct Biotechnol J* **21**, 495–505
6 (2023).

7 20. B. Kim, J. Lee, Y. Kim, S.-J. V. Lee, Regulatory systems that mediate the effects of temperature on
8 the lifespan of *Caenorhabditis elegans*. *J Neurogenet* **34**, 518–526 (2020).

9 21. C. Wang, B. Wang, T. Pandey, Y. Long, J. Zhang, F. Oh, J. Sima, R. Guo, Y. Liu, C. Zhang, S.
10 Mukherjee, M. Bassik, W. Lin, H. Deng, G. Vale, J. G. McDonald, K. Shen, D. K. Ma, A conserved
11 megaprotein-based molecular bridge critical for lipid trafficking and cold resilience. *Nat Commun*
12 **13**, 6805 (2022).

13 22. C. Wang, Y. Long, B. Wang, C. Zhang, D. K. Ma, GPCR signaling regulates severe stress-induced
14 organismic death in *Caenorhabditis elegans*. *Aging Cell* **22**, e13735 (2023).

15 23. W. Jiang, Y. Wei, Y. Long, A. Owen, B. Wang, X. Wu, S. Luo, Y. Dang, D. K. Ma, A genetic program
16 mediates cold-warming response and promotes stress-induced phenoptosis in *C. elegans*. *Elife* **7**
17 (2018).

18 24. J. Brunquell, S. Morris, Y. Lu, F. Cheng, S. D. Westerheide, The genome-wide role of HSF-1 in the
19 regulation of gene expression in *Caenorhabditis elegans*. *BMC Genomics* **17** (2016).

20 25. N. A. Baird, P. M. Douglas, M. S. Simic, A. R. Grant, J. J. Moresco, S. C. Wolff, J. R. Yates, G.
21 Manning, A. Dillin, HSF-1-mediated cytoskeletal integrity determines thermotolerance and life
22 span. *Science* **346**, 360–363 (2014).

23 26. R. Gomez-Pastor, E. T. Burchfiel, D. J. Thiele, Regulation of heat shock transcription factors and
24 their roles in physiology and disease. *Nat. Rev. Mol. Cell Biol.*, doi: 10.1038/nrm.2017.73 (2017).

25 27. R. I. Morimoto, The heat shock response: systems biology of proteotoxic stress in aging and
26 disease. *Cold Spring Harb Symp Quant Biol* **76**, 91–99 (2011).

27 28. V. Prahлад, T. Cornelius, R. I. Morimoto, Regulation of the Cellular Heat Shock Response in
28 *Caenorhabditis elegans* by Thermosensory Neurons. *Science* **320**, 811–814 (2008).

29 29. S. Charrin, S. Jouannet, C. Boucheix, E. Rubinstein, Tetraspanins at a glance. *J Cell Sci* **127**, 3641–
30 3648 (2014).

31 30. M. E. Hemler, Tetraspanin functions and associated microdomains. *Nat Rev Mol Cell Biol* **6**, 801–
32 811 (2005).

33 31. S. J. van Deventer, V.-M. E. Dunlock, A. B. van Spriel, Molecular interactions shaping the
34 tetraspanin web. *Biochem Soc Trans* **45**, 741–750 (2017).

35 32. M. Cui, M. Han, Roles of chromatin factors in *C. elegans* development. *WormBook*, 1–16 (2007).

1 33. C. González-Aguilera, F. Palladino, P. Askjaer, *C. elegans* epigenetic regulation in development and
2 aging. *Brief Funct Genomics* **13**, 223–234 (2014).

3 34. R. M. Woodhouse, A. Ashe, How do histone modifications contribute to transgenerational
4 epigenetic inheritance in *C. elegans*? *Biochem Soc Trans* **48**, 1019–1034 (2020).

5 35. Y. Shi, C. Mello, A CBP/p300 homolog specifies multiple differentiation pathways in *Caenorhabditis*
6 *elegans*. *Genes Dev* **12**, 943–955 (1998).

7 36. D. J. Eastburn, M. Han, A gain-of-function allele of *cbp-1*, the *Caenorhabditis elegans* ortholog of
8 the mammalian CBP/p300 gene, causes an increase in histone acetyltransferase activity and
9 antagonism of activated Ras. *Mol Cell Biol* **25**, 9427–9434 (2005).

10 37. M. Vora, M. Shah, S. Ostafi, B. Onken, J. Xue, J. Z. Ni, S. Gu, M. Driscoll, Deletion of microRNA-80
11 activates dietary restriction to extend *C. elegans* healthspan and lifespan. *PLoS Genet* **9**, e1003737
12 (2013).

13 38. L. Zhou, B. He, J. Deng, S. Pang, H. Tang, Histone acetylation promotes long-lasting defense
14 responses and longevity following early life heat stress. *PLoS Genet* **15**, e1008122 (2019).

15 39. D. S. Cabianca, C. Muñoz-Jiménez, V. Kalck, D. Gaidatzis, J. Padeken, A. Seeber, P. Askjaer, S. M.
16 Gasser, Active chromatin marks drive spatial sequestration of heterochromatin in *C. elegans*
17 nuclei. *Nature* **569**, 734–739 (2019).

18 40. A. Ganner, J. Gerber, A.-K. Ziegler, Y. Li, J. Kandzia, T. Matulenski, S. Kreis, G. Breves, M. Klein, G.
19 Walz, E. Neumann-Haefelin, CBP-1/p300 acetyltransferase regulates SKN-1/Nrf cellular levels,
20 nuclear localization, and activity in *C. elegans*. *Exp Gerontol* **126**, 110690 (2019).

21 41. L. D. Mathies, J. H. Lindsay, A. P. Handal, G. G. Blackwell, A. G. Davies, J. C. Bettinger, SWI/SNF
22 complexes act through CBP-1 histone acetyltransferase to regulate acute functional tolerance to
23 alcohol. *BMC Genomics* **21**, 646 (2020).

24 42. T. Y. Li, M. B. Sleiman, H. Li, A. W. Gao, A. Mottis, A. M. Bachmann, G. El Alam, X. Li, L. J. E.
25 Goeminne, K. Schoonjans, J. Auwerx, The transcriptional coactivator CBP/p300 is an evolutionarily
26 conserved node that promotes longevity in response to mitochondrial stress. *Nat Aging* **1**, 165–
27 178 (2021).

28 43. L. N. Barrett, S. D. Westerheide, The CBP-1/p300 Lysine Acetyltransferase Regulates the Heat
29 Shock Response in *C. elegans*. *Front Aging* **3**, 861761 (2022).

30 44. A. Shi, O. Liu, S. Koenig, R. Banerjee, C. C.-H. Chen, S. Eimer, B. D. Grant, RAB-10-GTPase-mediated
31 regulation of endosomal phosphatidylinositol-4,5-bisphosphate. *Proc Natl Acad Sci U S A* **109**,
32 E2306-2315 (2012).

33 45. N. Xu, S. O. Zhang, R. A. Cole, S. A. McKinney, F. Guo, J. T. Haas, S. Bobba, R. V. Farese, H. Y. Mak,
34 The FATP1-DGAT2 complex facilitates lipid droplet expansion at the ER-lipid droplet interface. *J
35 Cell Biol* **198**, 895–911 (2012).

1 46. R. Xiao, B. Zhang, Y. Dong, J. Gong, T. Xu, J. Liu, X. Z. S. Xu, A genetic program promotes *C. elegans*
2 longevity at cold temperatures via a thermosensitive TRP channel. *Cell* **152**, 806–817 (2013).

3 47. G. J. Lithgow, T. M. White, S. Melov, T. E. Johnson, Thermotolerance and extended life-span
4 conferred by single-gene mutations and induced by thermal stress. *Proc Natl Acad Sci U S A* **92**,
5 7540–7544 (1995).

6 48. D. Zhu, X. Wu, J. Zhou, X. Li, X. Huang, J. Li, J. Wu, Q. Bian, Y. Wang, Y. Tian, NuRD mediates
7 mitochondrial stress-induced longevity via chromatin remodeling in response to acetyl-CoA level.
8 *Sci Adv* **6**, eabb2529 (2020).

9 49. Y. Tian, G. Garcia, Q. Bian, K. K. Steffen, L. Joe, S. Wolff, B. J. Meyer, A. Dillin, Mitochondrial Stress
10 Induces Chromatin Reorganization to Promote Longevity and UPR(mt). *Cell* **165**, 1197–1208
11 (2016).

12 50. B. J. Oleson, J. Bhattrai, S. L. Zalubas, T. R. Kravchenko, Y. Ji, E. L. Jiang, C. C. Lu, C. R. Madden, J. G.
13 Coffman, D. Bazopoulou, J. W. Jones, U. Jakob, Early life changes in histone landscape protect
14 against age-associated amyloid toxicities through HSF-1-dependent regulation of lipid metabolism.
15 *Nat Aging*, doi: 10.1038/s43587-023-00537-4 (2023).

16 51. A. Olsen, M. C. Vantipalli, G. J. Lithgow, Lifespan extension of *Caenorhabditis elegans* following
17 repeated mild hormetic heat treatments. *Biogerontology* **7**, 221–230 (2006).

18 52. Z. Xu, Y. Hu, Y. Deng, Y. Chen, H. Hua, S. Huang, Q. Nie, Q. Pan, D. K. Ma, L. Ma, WDR-23 and SKN-
19 1/Nrf2 Coordinate with the BLI-3 Dual Oxidase in Response to Iodide-Triggered Oxidative Stress.
20 *G3 (Bethesda)* **8**, 3515–3527 (2018).

21 53. Z. Liu, H. Shi, J. Liu, The *C. elegans* TspanC8 tetraspanin TSP-14 exhibits isoform-specific localization
22 and function. *PLoS Genet* **18**, e1009936 (2022).

23 54. I. A. Nikonorova, J. Wang, A. L. Cope, P. E. Tilton, K. M. Power, J. D. Walsh, J. S. Akella, A. R.
24 Krauchunas, P. Shah, M. M. Barr, Isolation, profiling, and tracking of extracellular vesicle cargo in
25 *Caenorhabditis elegans*. *Curr Biol* **32**, 1924-1936.e6 (2022).

26 55. Y. Wang, Q. Yang, X. Meng, C. S. Wijaya, X. Ren, S. Xu, Recruitment of tetraspanin TSP-15 to
27 epidermal wounds promotes plasma membrane repair in *C. elegans*. *Dev Cell* **57**, 1630-1642.e4
28 (2022).

29 56. Y. Jin, Y. Takeda, Y. Kondo, L. P. Tripathi, S. Kang, H. Takeshita, H. Kuhara, Y. Maeda, M.
30 Higashiguchi, K. Miyake, O. Morimura, T. Koba, Y. Hayama, S. Koyama, K. Nakanishi, T. Iwasaki, S.
31 Tetsumoto, K. Tsujino, M. Kuroyama, K. Iwahori, H. Hirata, T. Takimoto, M. Suzuki, I. Nagatomo, K.
32 Sugimoto, Y. Fujii, H. Kida, K. Mizuguchi, M. Ito, T. Kijima, H. Rakugi, E. Mekada, I. Tachibana, A.
33 Kumanogoh, Double deletion of tetraspanins CD9 and CD81 in mice leads to a syndrome
34 resembling accelerated aging. *Sci Rep* **8**, 5145 (2018).

35 57. C. Zhang, M. B. Lai, M. G. Pedler, V. Johnson, R. H. Adams, J. M. Petrash, Z. Chen, H. J. Junge,
36 Endothelial Cell-Specific Inactivation of TSPAN12 (Tetraspanin 12) Reveals Pathological
37 Consequences of Barrier Defects in an Otherwise Intact Vasculature. *Arterioscler Thromb Vasc Biol*
38 **38**, 2691–2705 (2018).

1 58. J. Franz, M. Tarantola, C. Riethmüller, How tetraspanins shape endothelial and leukocyte nano-
2 architecture during inflammation. *Biochem Soc Trans* **45**, 999–1006 (2017).

3 59. S. Brenner, The genetics of *Caenorhabditis elegans*. *Genetics* **77**, 71–94 (1974).

4 60. J. Schindelin, I. Arganda-Carreras, E. Frise, V. Kaynig, M. Longair, T. Pietzsch, S. Preibisch, C.
5 Rueden, S. Saalfeld, B. Schmid, J.-Y. Tinevez, D. J. White, V. Hartenstein, K. Eliceiri, P. Tomancak, A.
6 Cardona, Fiji - an Open Source platform for biological image analysis. *Nat Methods* **9**,
7 10.1038/nmeth.2019 (2012).

8

9

10 **Acknowledgments:** Some strains were provided by the *Caenorhabditis* Genetics Center
11 (CGC), which is funded by the NIH Office of Research Infrastructure Programs (P40
12 OD010440).

13 **Funding:** The work was supported by NIH grants (R35GM139618 to D.K.M. and
14 R35GM118167 to O.D.W.), BARI Investigator Award (D.K.M.) and UCSF PBBR New Frontier
15 Research Award (D.K.M.).

16 **Author Contributions:**

17 Conceptualization: WIJ, ODW, DKM

18 Methodology: WIJ, HDB, BW, AW, MK, FO, JD, XH, SG

19 Investigation: WIJ, HDB, BW, AW, MK, FO, JD, XH, SG, ODW, DKM

20 Visualization: WIJ, HDB, ODW, DKM

21 Supervision: ODW, DKM

22 Writing—original draft: WIJ, DKM

23 Writing—review & editing: WIJ, HDB, BW, AW, MK, FO, JD, XH, SG, ODW, DKM

24 **Competing Interests:** The authors declare that they have no competing interests.

25 **Data and Materials Availability:** All data needed to evaluate the conclusions in the
26 paper are present in the paper and/or the Supplementary Materials.

27

28 **Table of contents for supplementary materials**

29 Fig. S1-S9

1 Table S1

2 Table S2

3 Movie S1

4

5 **Figure captions**

6 **Fig. 1. Thermal stress induces TSP-1 expression and tetraspanin web-like structure**

7 **formation.** (A) Representative bright field and epifluorescence images showing expression of
8 an integrated transgene *tsp-1p::tsp-1::GFP* under temperatures and durations indicated. Scale
9 bars: 100 μ m. (B) Quantification of TSP-1::GFP fluorescence intensities under conditions
10 indicated. *** indicates $P < 0.001$ ($n > 40$ animals per condition). (C) Schematic of the *tsp-1*
11 gene structure, predicted membrane topology (by DeepTMHMM) and structure (by AlphaFold2)
12 of TSP-1. (D) SDS-PAGE and native-PAGE western blots showing heat-induced increase in
13 abundance and formation of dimers and multimers (asterisk) by TSP-1::GFP. (E)
14 Representative confocal fluorescence images showing high-resolution Z-stack views of
15 tetraspanin web structure formed by TSP-1::GFP, with enlarged view at right bottom. Scale
16 bars: 10 μ m.

17 **Fig. 2. Expression and roles of TSP-1 in membrane barrier integrity in adults and during**

18 **aging.** (A-D) Representative epifluorescence images showing TSP-1::GFP up-regulation from
19 L4 (A) to young adults (B) and during aging (C-D). (E) Quantification of fluorescence intensities
20 of TSP-1::GFP under conditions indicated. *** indicates $P < 0.001$ ($n > 30$ animals per
21 condition). (F) Schematic of the assay for acute membrane barrier functions. (G) Quantification
22 of intensities of fluorescein accumulated by live animals under conditions indicated. *** indicates
23 $P < 0.001$ ($n > 20$ animals per condition). (H-J) Representative epifluorescence images showing
24 fluorescein accumulation in animals of indicated stages, temperature and genotypes (wild type
25 and *tsp-1* deletion mutant allele *ok3594*). Scale bars: 100 μ m.

1

2 **Fig. 3. Early-life thermal stress-triggered TSP-1::GFP is long-lasting and requires CBP-1.**

3 (A) Representative epifluorescence images showing long-lasting up-regulation of TSP-1::GFP
4 upon transient early-life thermal stress (ELTS, T28 for 24 hrs at L4). (B) Representative
5 epifluorescence images showing up-regulation of TSP-1::GFP upon sustained thermal stress
6 (T28 for 24, 48 or 72 hrs starting at L4). (C) Quantification of fluorescence intensities of TSP-
7 1::GFP under conditions indicated. *** indicates $P < 0.001$ ($n > 30$ animals per condition). (D)
8 Schematic of experimental flow using RNAi screen to identify genes required for ELTS induction
9 of TSP-1::GFP. (E) Representative bright-field and epifluorescence images showing that RNAi
10 against *tsp-1* or *cbp-1* blocks up-regulation of TSP-1::GFP by ELTS. (F) Quantitative RT-PCR
11 measurements of *tsp-1* expression levels under conditions indicated, showing transient *tsp-1*
12 up-regulation by ELTS in a CBP-1-dependent manner. *** indicates $P < 0.001$ (three
13 independent biological replicates). Scale bars: 100 μ m.

14 **Fig. 4. Subcellular localization and stability of tetraspanin web formed by endogenous**

15 **TSP-1::wrnScarlet.** (A) Representative confocal images showing co-localization of the marker
16 Akt-PH::GFP, which binds to intestinal apical plasma membrane inner leaflet PIP2/3, with
17 endogenous TSP-1 tagged with wrnScarlet by CRISPR. (B) Fluorescent intensity correlation
18 analysis showing close proximity of Akt-PH::GFP and TSP-1::wrnScarlet. (C) Representative
19 confocal images showing non-co-localization of the marker ERm::GFP, which labels intestinal
20 ER membrane, with endogenous TSP-1 tagged with wrnScarlet by CRISPR. Scale bars: 10
21 μ m. (D) Fluorescent intensity correlation analysis for ERm::GFP and TSP-1::wrnScarlet. (E)
22 Representative confocal time-series images showing stability of tetraspanin webs formed by
23 endogenous TSP-1::wrnScarlet, with enlarged views in (F). Scale bars: 10 μ m.

24 **Fig. 5. Early-life thermal stress-triggered thermal resilience and longevity requires TSP-1.**

25 (A) Lifespan curves of wild type and *tsp-1* mutants at 28 °C starting at L4.20% median and 28%

1 maximal survival decrease in *tsp-1* mutants *** indicates $P < 0.001$ (n > 40 animals per
2 condition). (B) Lifespan curves of wild type and *tsp-1* mutants at constant 20 °C or after transient
3 28 °C for 24 hrs at L4 (ELTS). 36% median and 20% maximal lifespan extension by ELTS in
4 wild type, $p=0.0008$. *** indicates $P < 0.001$ (n > 35 animals per condition). (C) Lifespan curves
5 of wild type and *tsp-1* mutants at 28 °C after transient 28 °C for 24 hrs at L4 (ELTS) . 33%
6 median and 33% maximal survival decrease in *tsp-1* mutants *** indicates $P < 0.001$ (n > 35
7 animals per condition). (D) Lifespan curves of wild type animals with RNAi against *cbp-1* or
8 control at 28 °C starting at L4. 80% median and 50% maximal survival decrease with RNAi
9 against *cbp-1*. *** indicates $P < 0.001$ (n > 40 animals per condition) (E) Representative
10 confocal fluorescence images showing ELTS-induced increase in numbers of nuclei with
11 GFP::CBP-1 in the posterior intestine. (F) Quantification of numbers of nuclei with GFP::CBP-1
12 in the posterior intestine under conditions indicated. (G) Model of how ELTS induces lasting
13 organismal thermal resilience through HSF-independent epigenetic regulation of TSP-1 and
14 stable tetraspanin web structure formation.

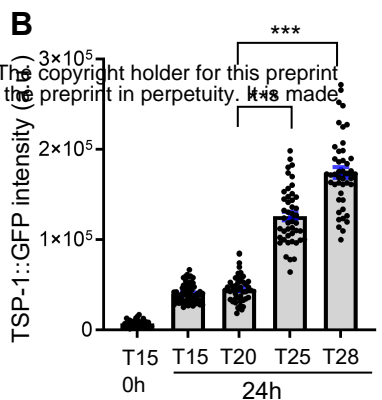
15 **Fig. 6. Gain-of-function of TSP-1 confers longevity extension in *C. elegans* and thermal
16 resilience in human cells.** (A) Schematic of the transgene that produces *tsp-1* gain-of-function
17 over-expression lines (OE line 1 at low level, OE line 2 at high level as measured by qRT-PCR).
18 *** indicates $P < 0.001$.(B) Lifespan curves of wild type and two representative *tsp-1* OE lines at
19 28 °C starting at L4. 50% median and 16% maximal survival extension by overexpression of *tsp-
20 1* in wild type, *** indicates $P < 0.001$ (n > 40 animals per condition). (C) Lifespan curves of wild
21 type and *tsp-1* OE lines at constant 20 °C. 63% median and 24% maximal lifespan extension by
22 overexpression of *tsp-1* in wild type, *** indicates $P < 0.001$ (n > 40 animals per condition). (D)
23 Serial confocal fluorescence images showing tetraspanin web-like structures formed in the
24 human cell line HEK293 by CMV promoter-driven expression of *C. elegans tsp-1::GFP* (bottom)
25 but not *GFP* alone (top). Scale bars: 10 μ m. (E) Quantification of survival rates after heat shock

- 1 in HEK293 cells showing enhanced thermal resilience conferred by ectopic gain-of-function of
- 2 *C. elegans* TSP-1::GFP. *** indicates $P < 0.001$ (three independent biological replicates).

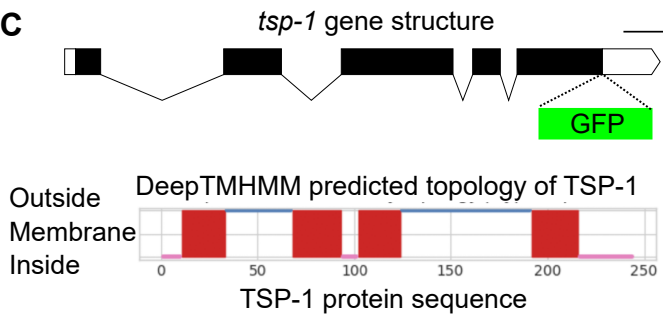
A

Integrated translational reporter *tsp-1p::tsp-1::GFP*

bioRxiv preprint doi: <https://doi.org/10.1101/203425.550452>; this version posted December 17, 2017. The copyright holder for this preprint (which was not certified by peer review) is the author/funder, who has granted bioRxiv a license to display the preprint in perpetuity. It is made available under aCC-BY-NC-ND 4.0 International license.

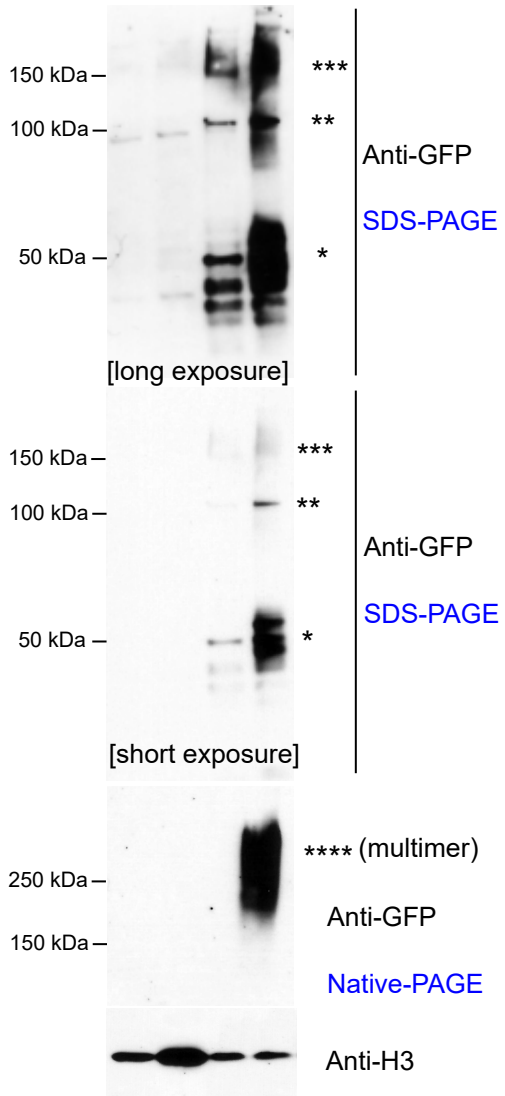


C

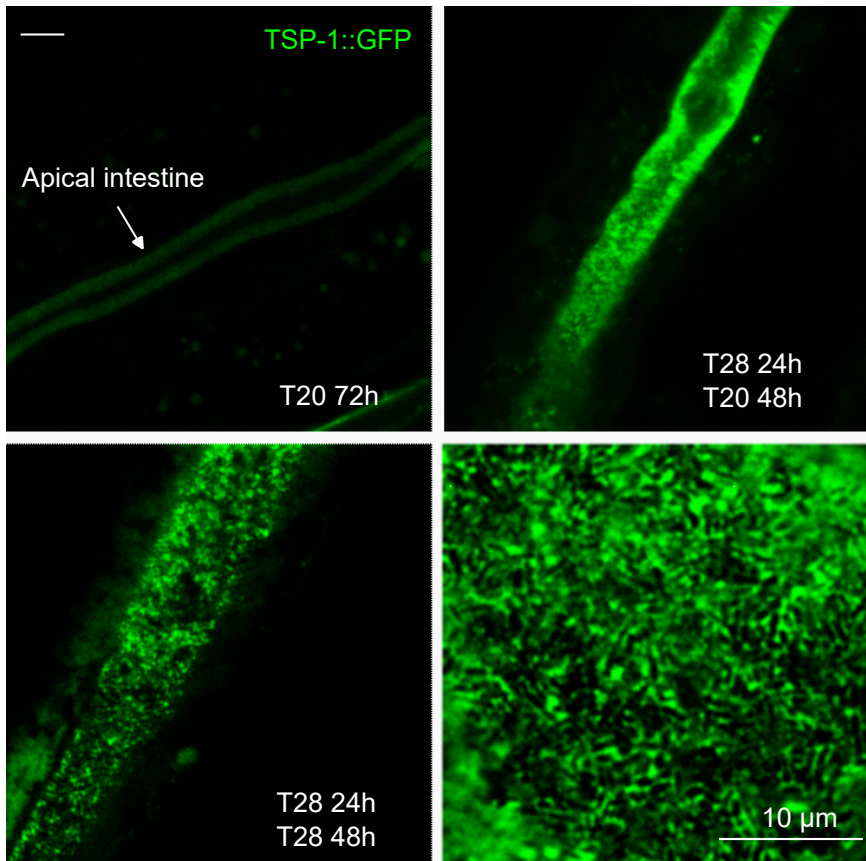


D Wild TSP-1

T28 - + - +



E

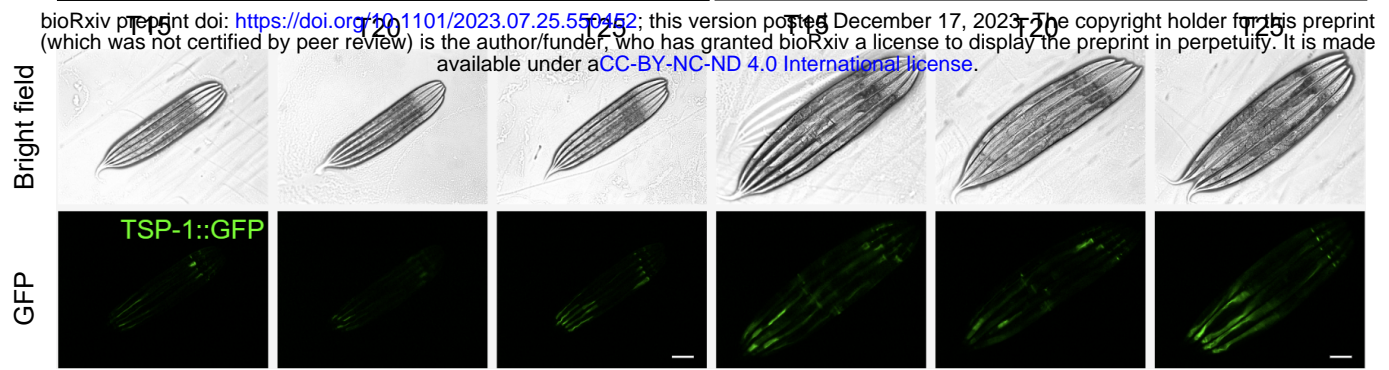


A

L4 stage

B

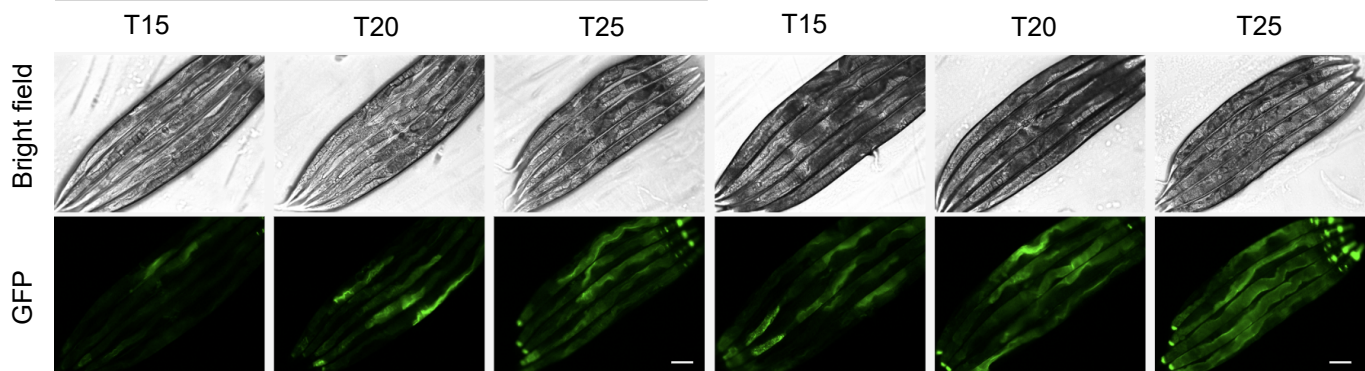
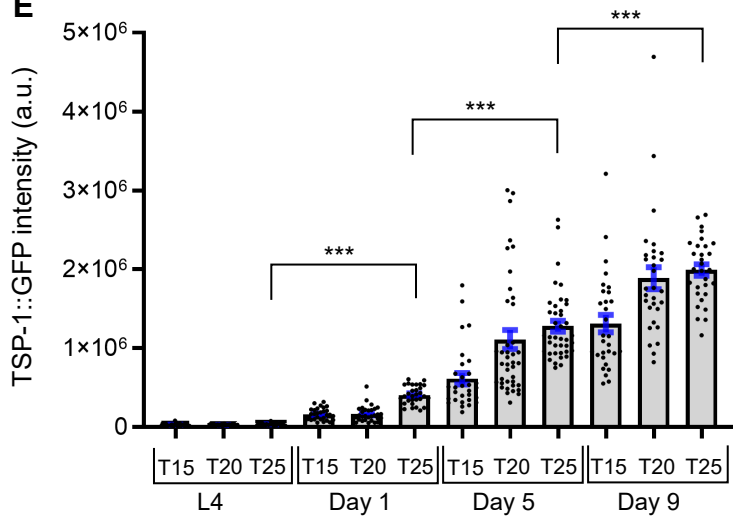
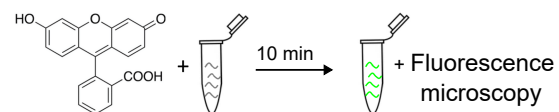
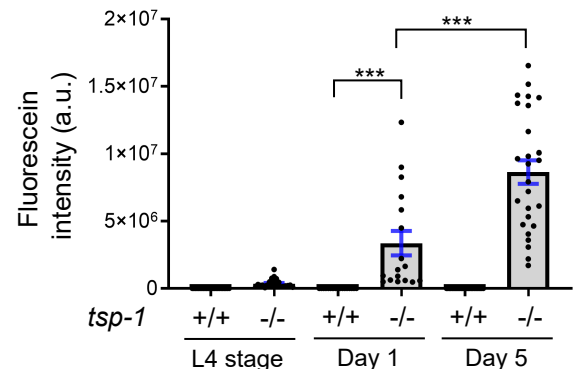
Day 1 (24h post L4)

**C**

Day 5 (120h post L4)

D

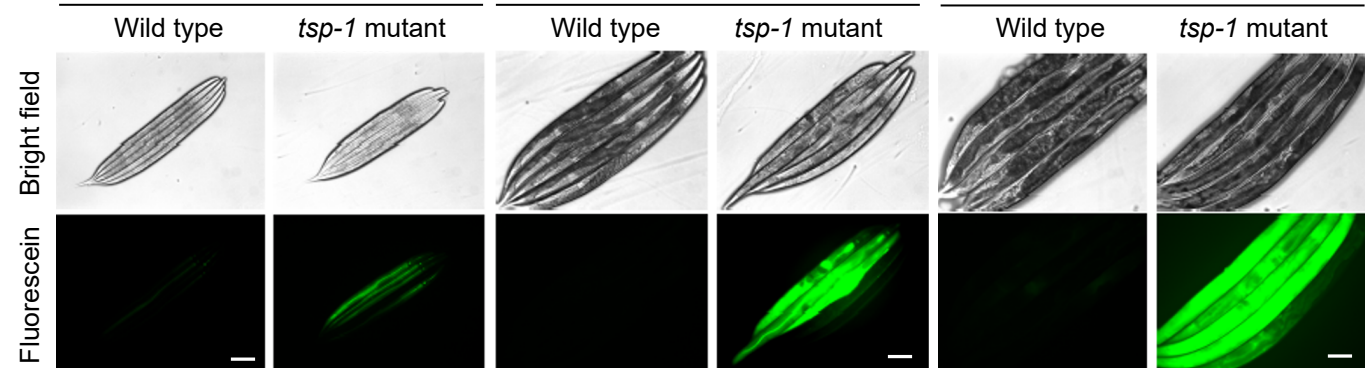
Day 9 (216h post L4)

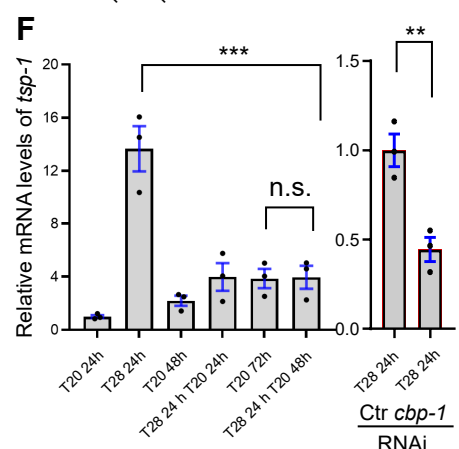
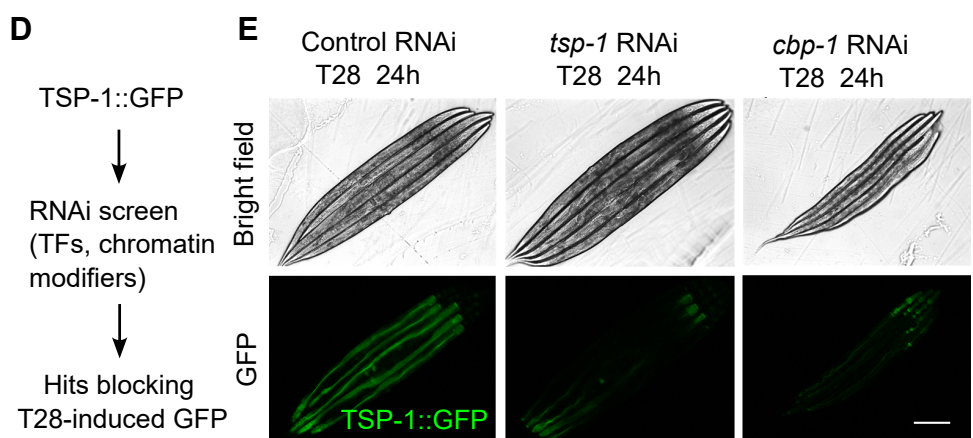
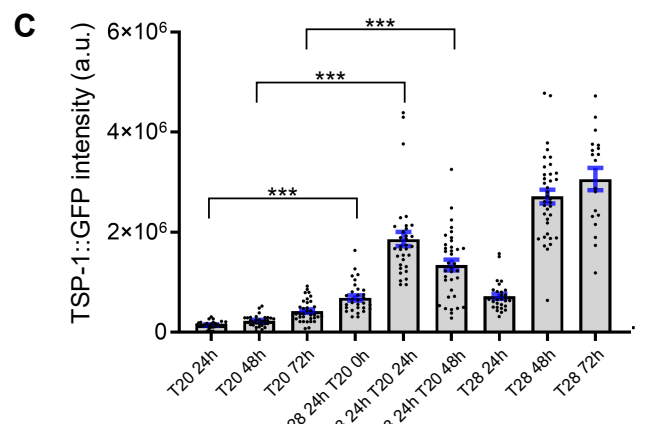
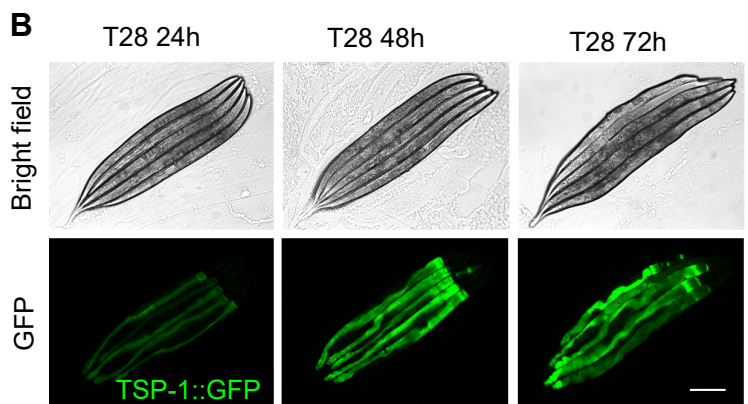
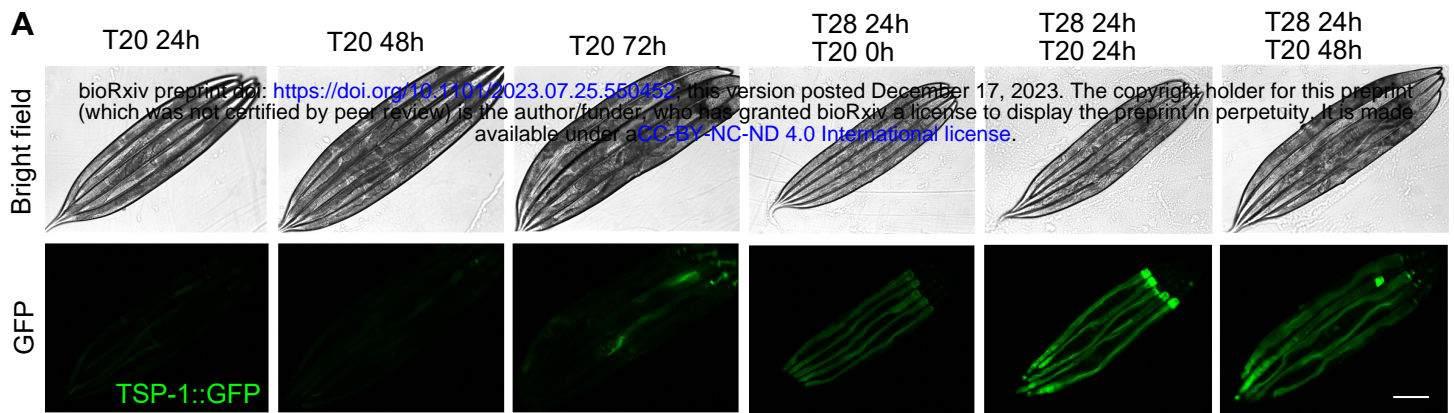
**E****F** Assay for acute membrane barrier functions:**G****H**

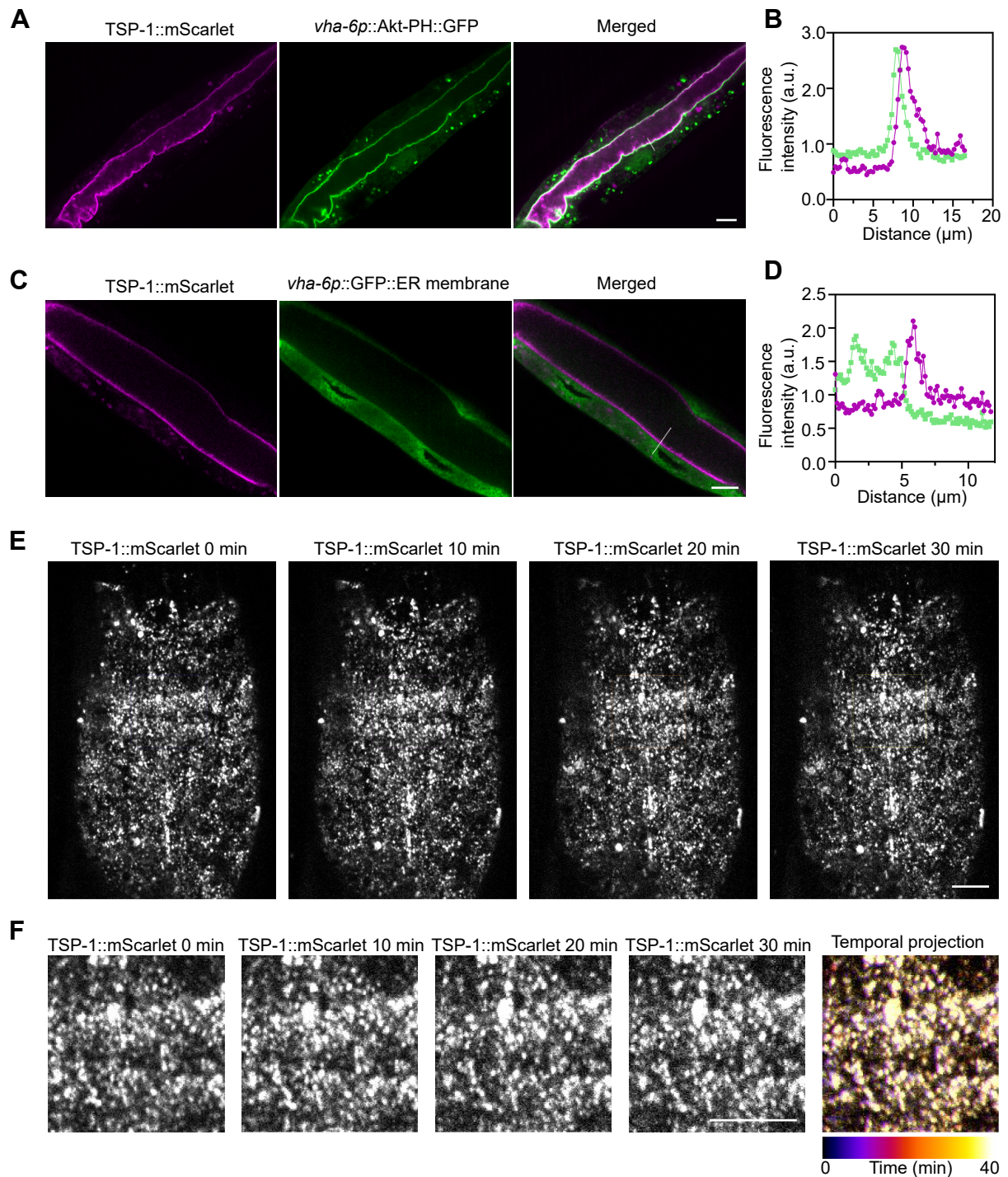
L4 stage (T20)

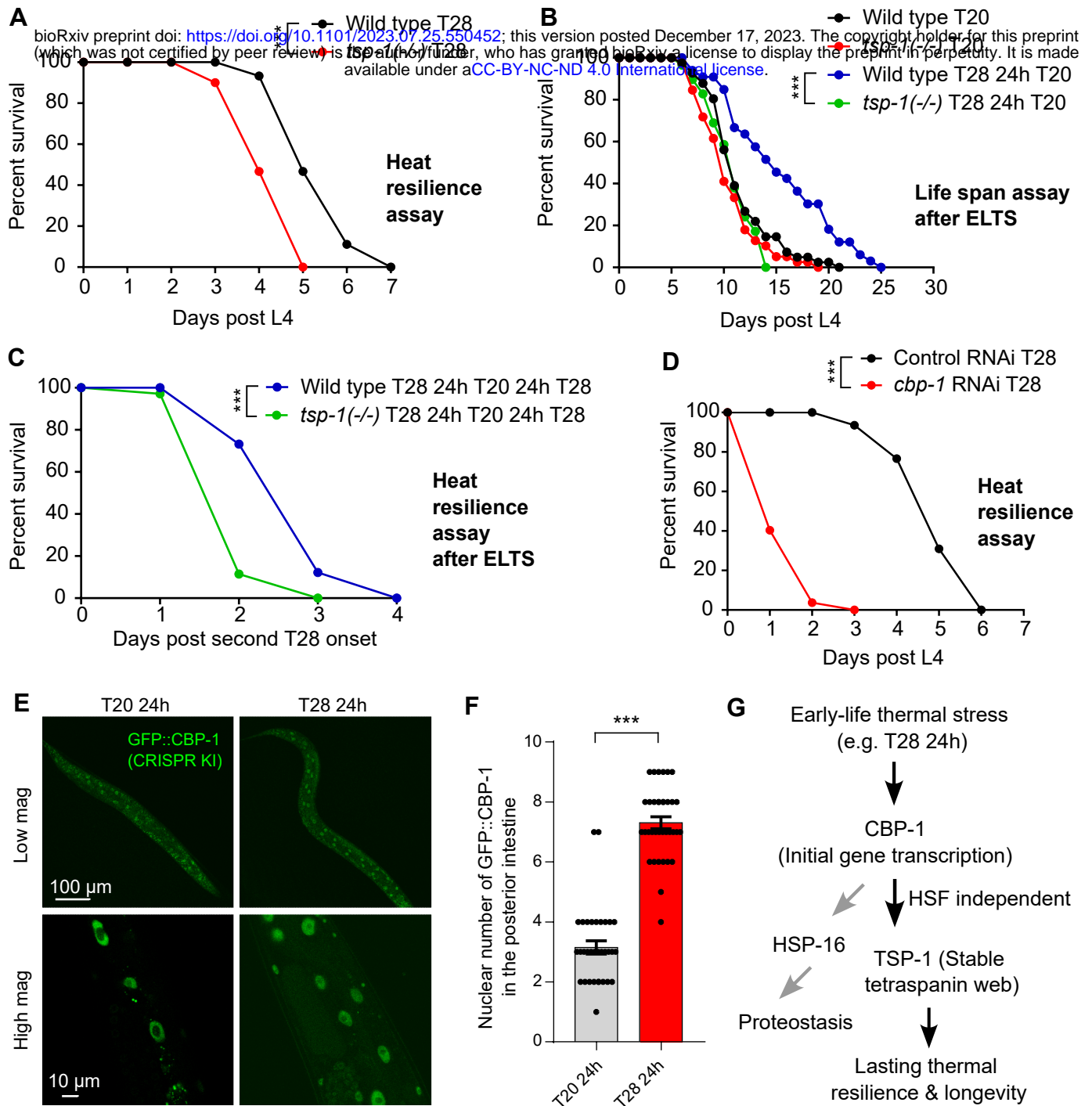
Day 1 (T20)

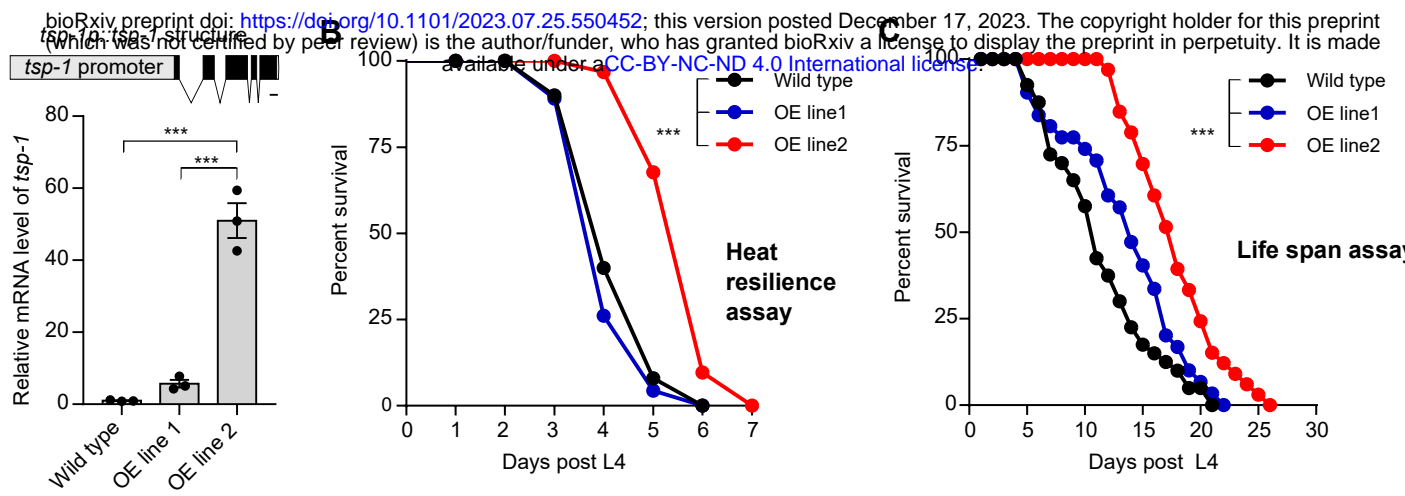
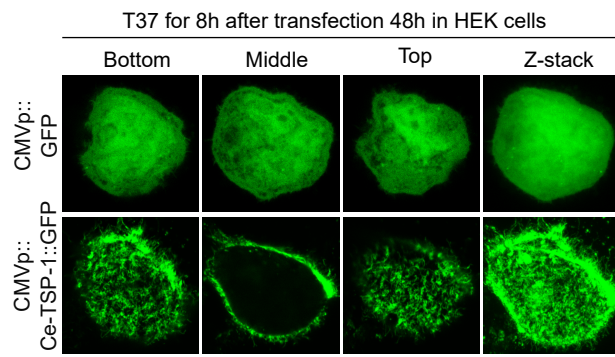
Day 5 (T20)



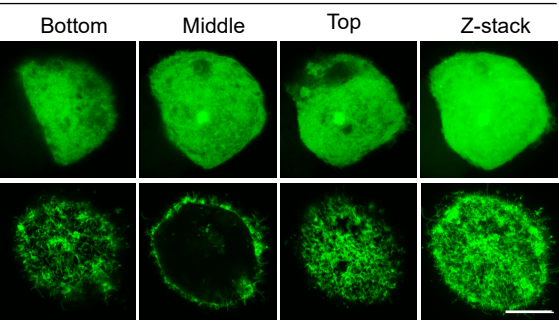
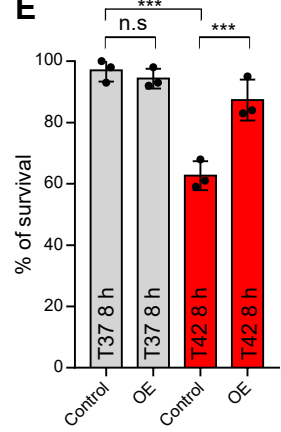






A**D**

T42 for 8h after transfection 48h in HEK cells

**E**

Science Advances

AAAS

Supplementary Materials for

Early-life stress triggers long-lasting organismal resilience and longevity via tetraspanin

Wei I. Jiang *et al.*

*Corresponding author. Email: Dengke.Ma@ucsf.edu

This PDF file includes:

figs. S1 to S9

Other Supplementary Materials for this manuscript include the following:

Table S1

Table S2

Movies S1

Supplemental Figures

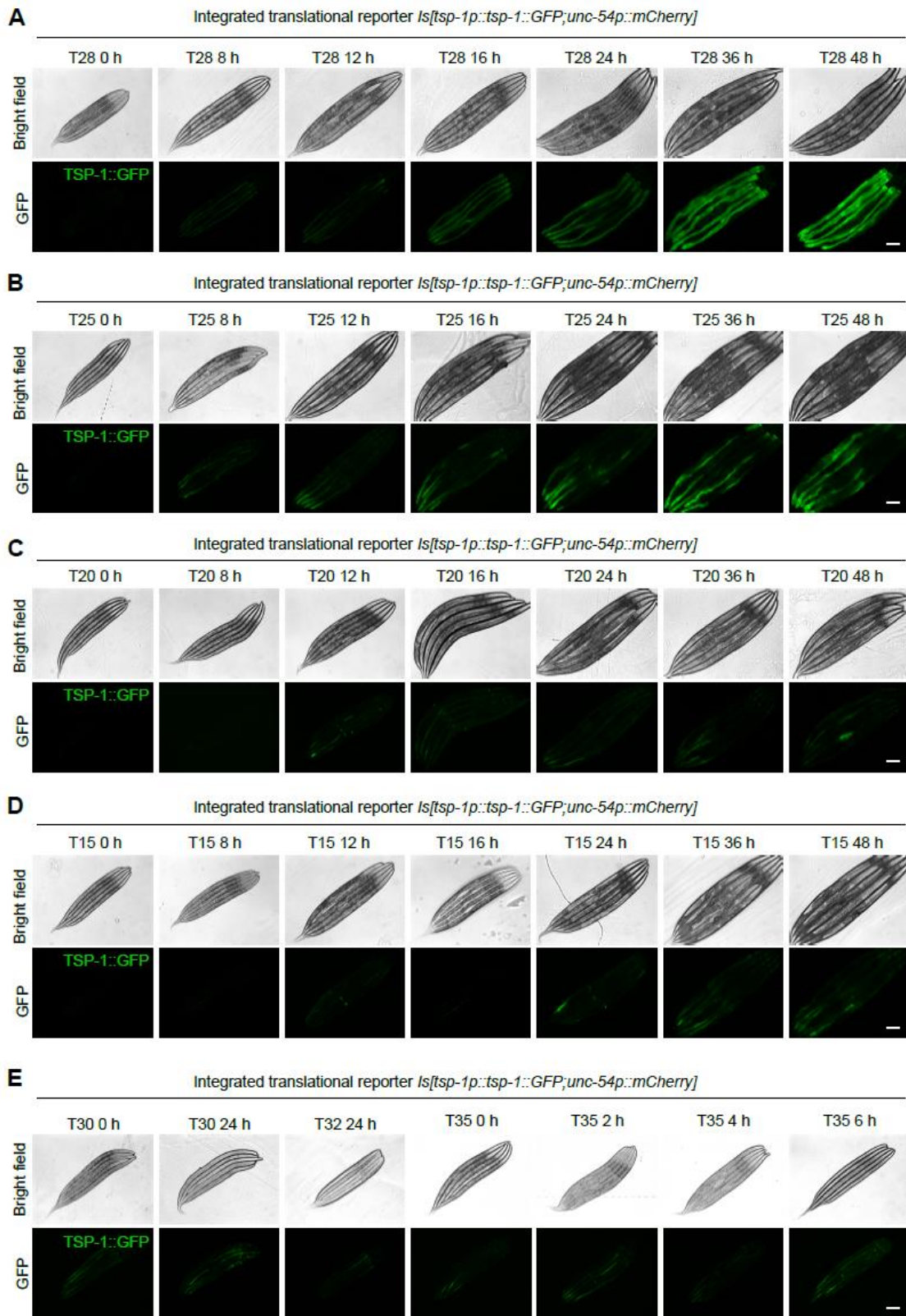


fig. S1. Duration and temperature-dependent induction of TSP-1::GFP. (A-E)

Representative bright-field and epifluorescence images showing expression of *tsp-1p::tsp-1::GFP* under temperatures and durations indicated. Scale bars: 100 μ m.

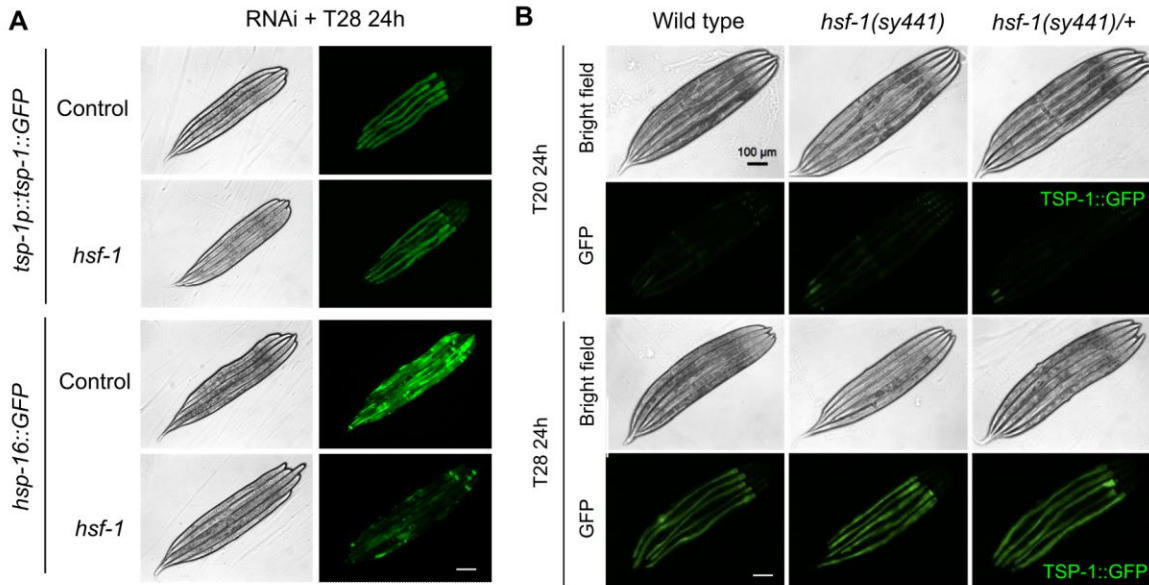


fig. S2. TSP-1 induction by T28 is independent of HSF-1. (A) Representative bright-field and epifluorescence images showing expression of *tsp-1p::tsp-1::GFP* or *hsp-16p::GFP* at 28 °C for 24 hrs, with control and RNAi against *hsf-1*. (B) Representative bright-field and epifluorescence images showing expression of *tsp-1p::tsp-1::GFP* at 28 °C for 24 hrs in wild type, *hsf-1(sy441)* reduction-of-function heterozygous or homozygous mutants. Scale bars: 100 μm.

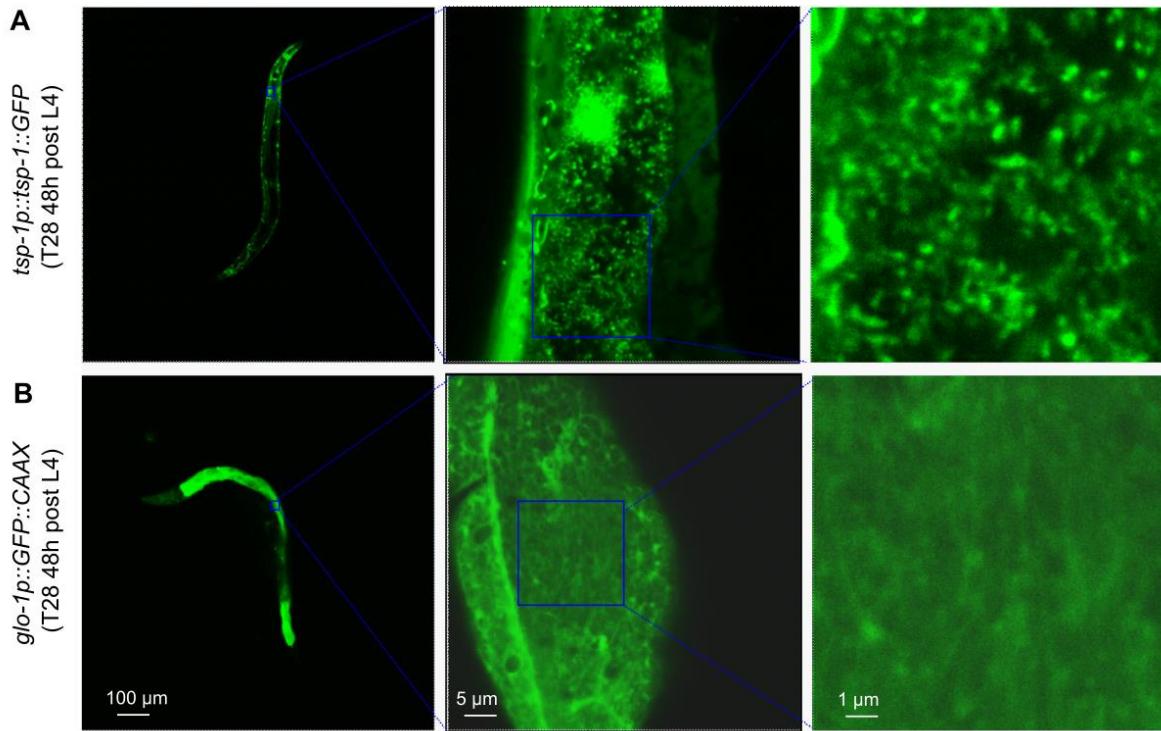


fig. S3. Tetraspanin web regulation by heat is specific for TSP-1. (A) Representative confocal fluorescence images showing T28-induced tetraspanin web structure formation by *tsp-1p::tsp-1::GFP* transgenes. (B), Representative confocal fluorescence images showing intestinal membrane GFP from *glo-1p::GFP::CAAX* under identical conditions (T28 48 hrs).

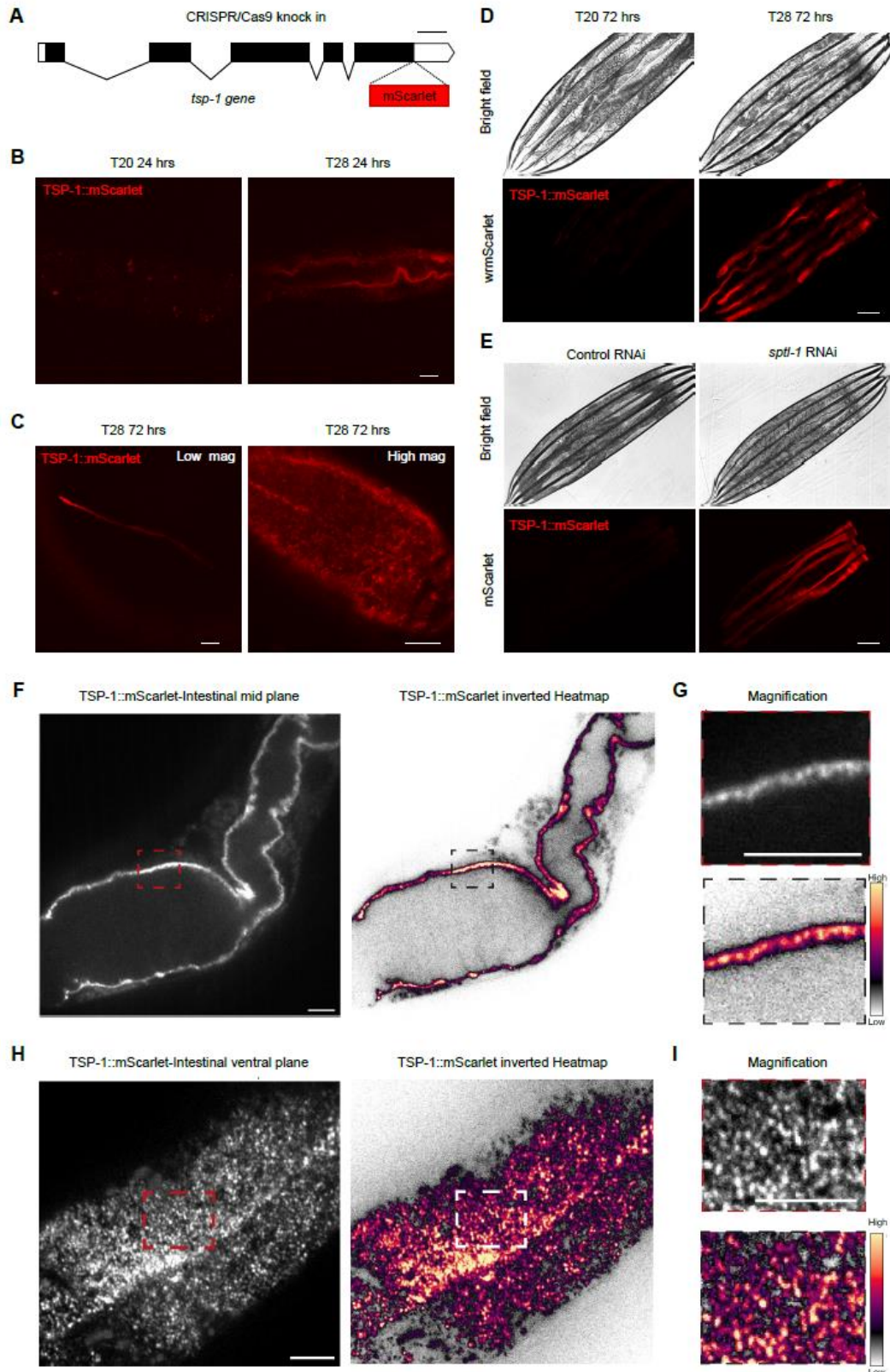


fig. S4. Heat-induced *tsp-1* endogenously tagged with wrmScarlet. (A) Schematic of *tsp-1* gene structure showing CRISPR-mediated knock-in of wrmScarlet at the C-terminus of TSP-1. (B) Representative confocal fluorescence images showing up-regulation of endogenous TSP-1::wrmScarlet by 28 °C for 24 hrs. (C) Representative confocal fluorescence images showing low and high-mag views of endogenous TSP-1::wrmScarlet induced by 28 °C for 72 hrs. (D) Representative epifluorescence images showing up-regulation of endogenous TSP-1::wrmScarlet by 28 °C for 72 hrs. (E) Representative epifluorescence images showing up-regulation of endogenous TSP-1::wrmScarlet by RNAi against *sptl-1*, loss of which disrupts the biosynthesis of sphingolipids mimicking heat-induced membrane effects. (F-I) Representative spinning disc confocal images showing high-resolution views of tetraspanin web structures.

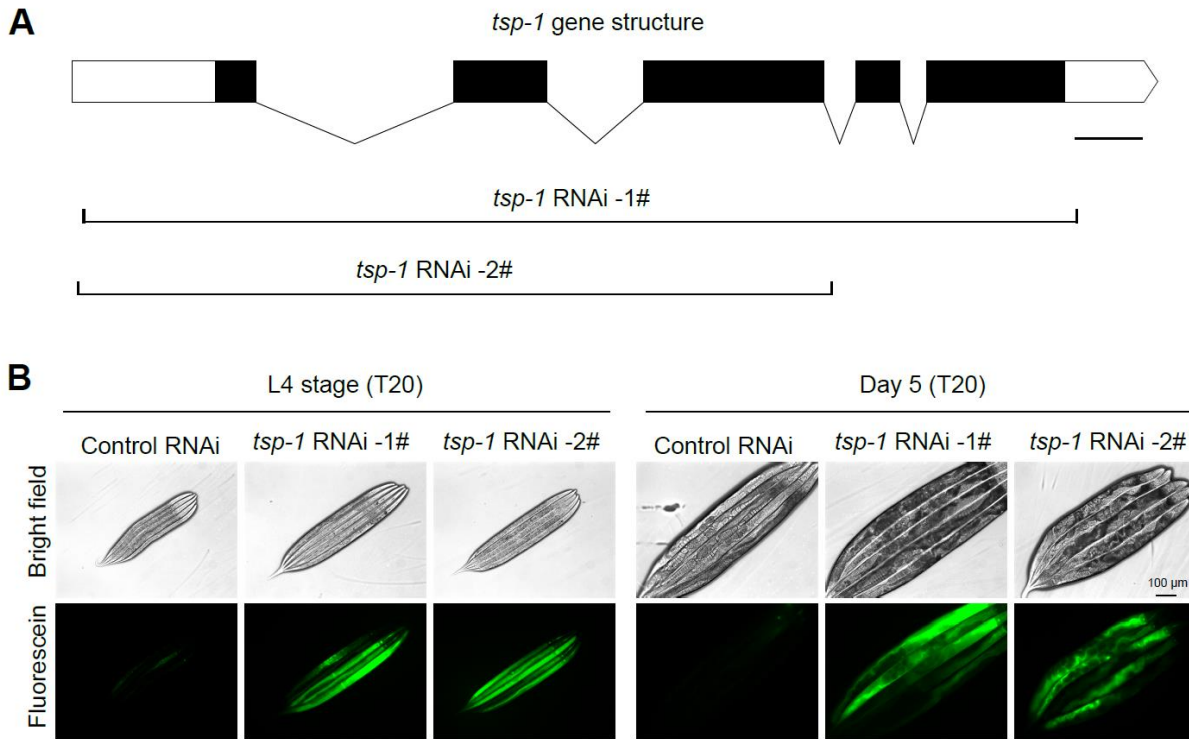


fig. S5. RNAi against *tsp-1* recapitulates mutant phenotype in membrane barrier functions.

(A) Schematic of *tsp-1* gene structure showing two genomic regions used to construct RNAi for expression in *E. Coli* and feeding to *C. elegans*. (B) Representative epifluorescence images showing enhanced fluorescein uptake in *tsp-1* RNAi-treated animals, at both L4 stage and Day 5-old animals. Scale bars: 100 μm.

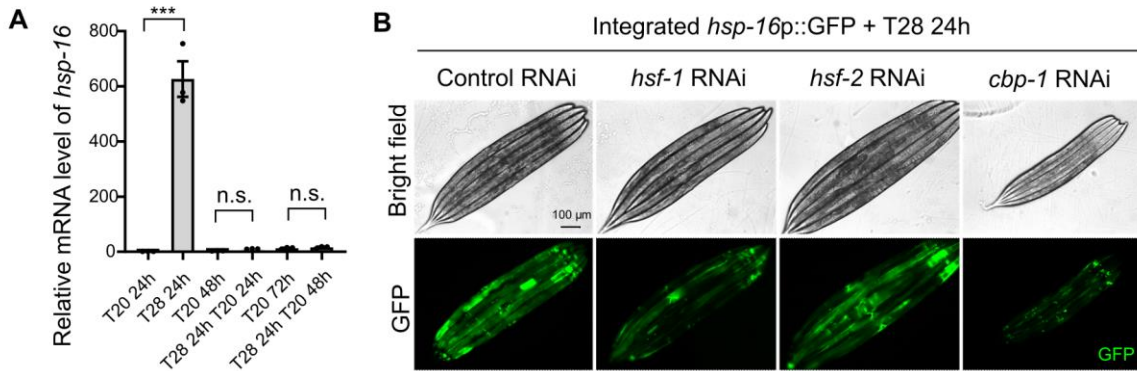


fig. S6. Heat shock protein induction by T28 requires both HSF-1 and CBP-1. (A)

Quantitative RT-PCR measurements of *hsp-16* expression levels showing its transient induction by ELTS (T28 for 24 hrs at L4). *** indicates $P < 0.001$ (three independent biological replicates). (B) Representative epifluorescence images of animals with RNAi against *hsf-1* or *cbp-1* showing up-regulation of *hsp-16p::GFP* by ELTS that depends on both HSF-1 and CBP-1, but not HSF-2. Scale bars: 100 μ m.

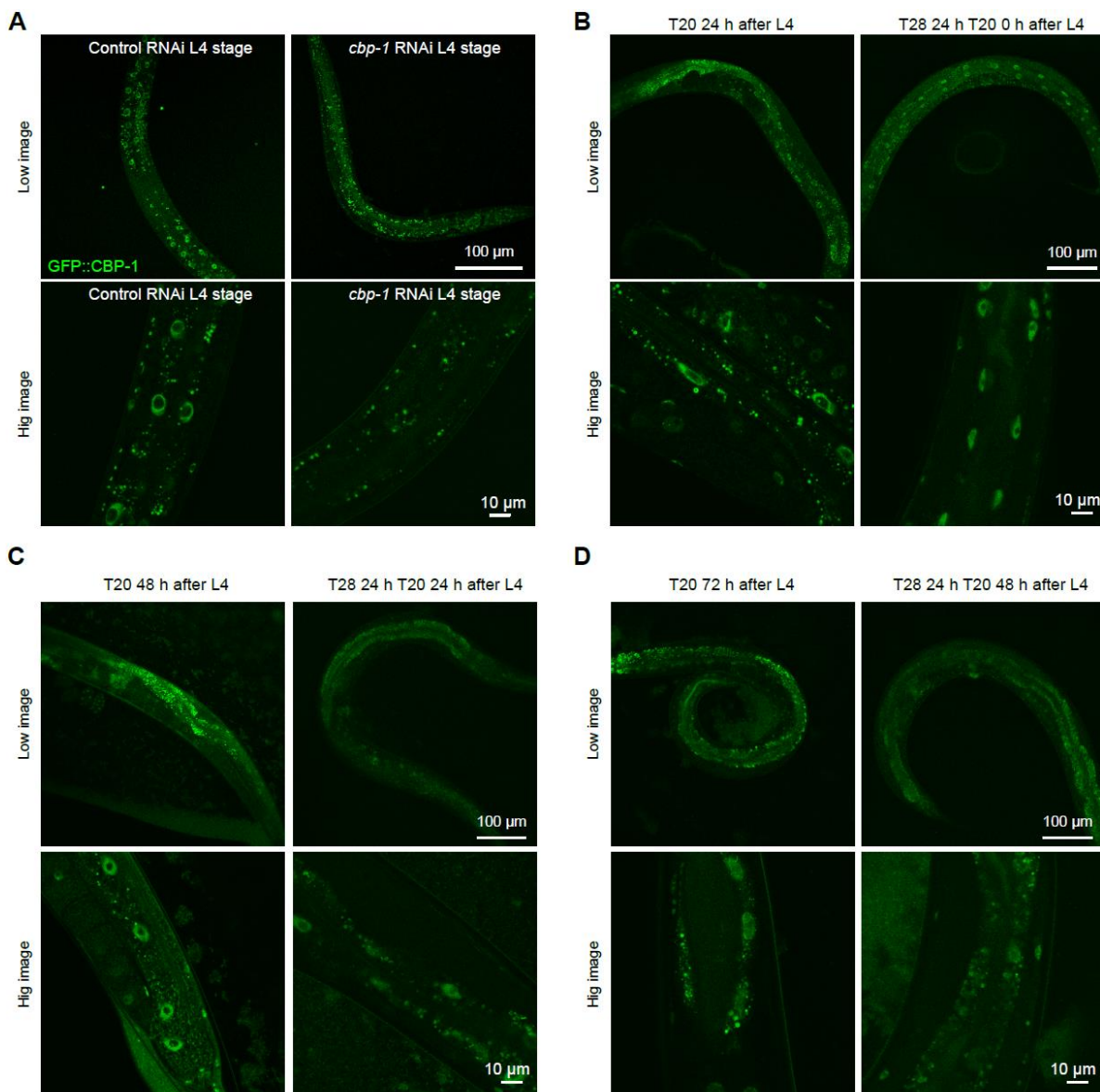


fig. S7. Heat-induced nuclear entry of CBP-1 endogenously tagged with GFP. (A)
Representative confocal fluorescence images showing specific nuclear signals of GFP::CBP-1 (by CRISPR knock-in at the endogenous *cbp-1* locus) that were diminished by RNAi against *cbp-1*. **(B)** Representative confocal fluorescence images showing increased nuclear entry of endogenous GFP::CBP-1 by 28 °C for 24 hrs. **(C)** Representative confocal fluorescence images showing unaltered GFP::CBP-1 by 28 °C for 24 hrs and 20 °C for 24 hrs. **(D)** Representative

confocal fluorescence images showing unaltered GFP::CBP-1 by 28 °C for 24 hrs and 20 °C for 48 hrs. Shown are both high and low-magnification views. Scale bars are indicated.

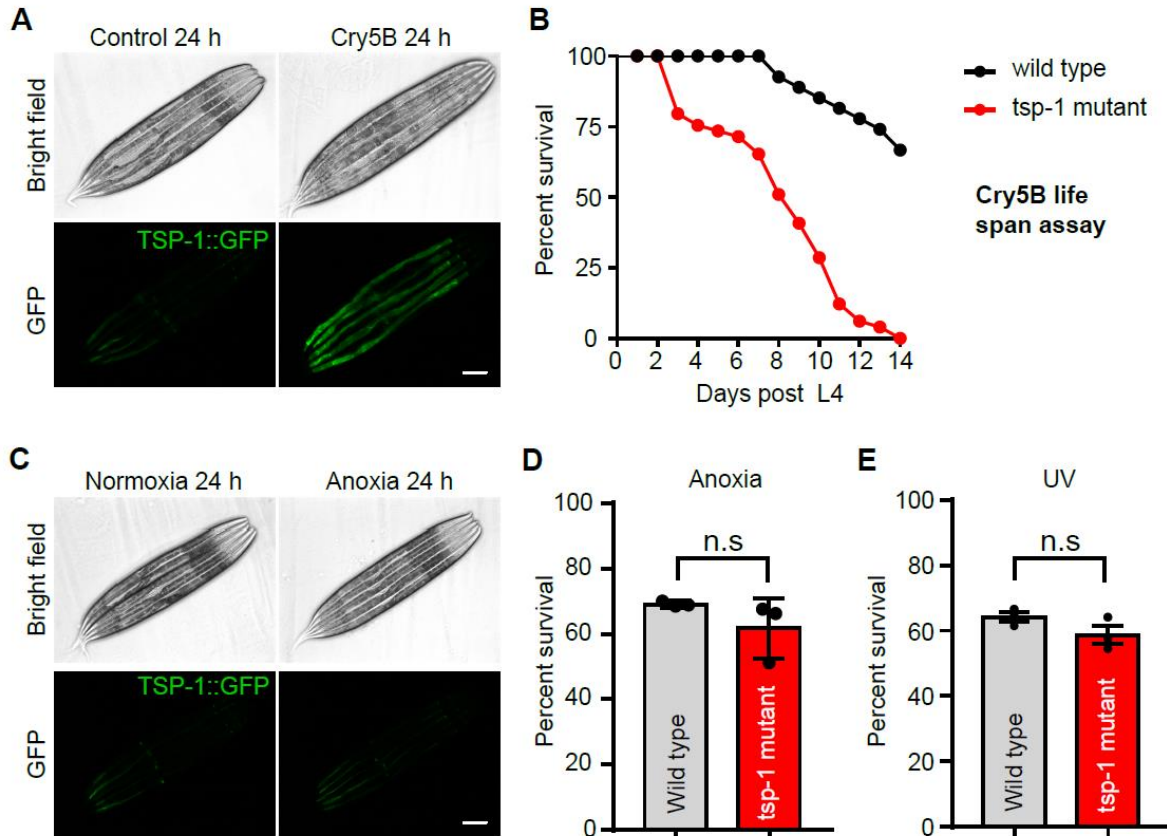


fig S8. Cry5B, UV, and anoxia effects on TSP-1 and organismal stress resilience. (A) Representative brightfield and epifluorescence images showing expression of an integrated transgene *tsp-1p::tsp-1::GFP* treated with cry5B expressing bacteria or control. Scale bars: 100 μ m. (B) Lifespan curves of wild type and *tsp-1* deletion mutant allele *ok3594* with cry5B or control starting at L4. (C) Representative bright field and epifluorescence images showing expression of an integrated transgene *tsp-1p::tsp-1::GFP* under normoxia or anoxia for 24 h. Scale bars: 100 μ m. (D) Percentage survival of wild type and *tsp-1* deletion mutants after exposure to anoxia at L4. (E) Percentage survival of wild type and *tsp-1* deletion mutants after exposure to UV at L4.

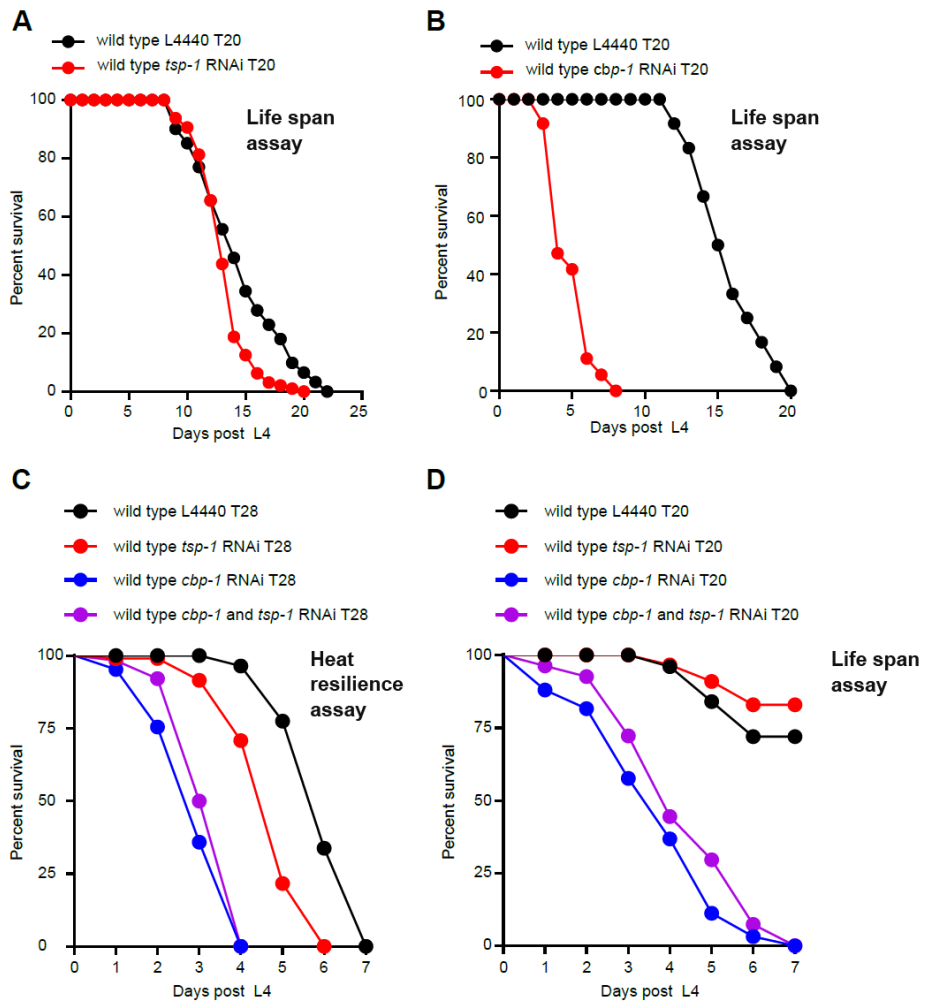


fig S9. Effects of co-application of *cbp-1* RNAi and *tsp-1* RNAi in *C. elegans*. (A) Lifespan curves of wild type with *tsp-1* RNAi or control starting at L4. (B) Lifespan curves of wild type with *cbp-1* RNAi or control at constant 20 °C. (C) Lifespan curves of wild type with *tsp-1* RNAi, *cbp-1* RNAi or *tsp-1*+*cbp-1* RNAi exposure to 28 °C starting at L4. (D) Lifespan curves of wild type with *tsp-1* RNAi, *cbp-1* RNAi or *tsp-1*+*cbp-1* RNAi at constant 20 °C starting at L4.

Table S1.

Customized RNAi screen for candidate nuclear regulators of heat-induced TSP-1::GFP.

Table S2.

Quantitative summary of lifespan assay statistics and results.

Movie S1.

Tetraspanin webs exhibit stability from 120-min imaging of TSP-1::mScarlet. Scale bar: 10 μ m.